

# AcuA: the AKARI/IRC Mid-infrared Asteroid Survey

Fumihiko USUI<sup>1</sup>, Daisuke KURODA<sup>2</sup>, Thomas G. MÜLLER<sup>3</sup>, Sunao HASEGAWA<sup>1</sup>, Masateru ISHIGURO<sup>4</sup>,  
Takafumi OOTSUBO<sup>5</sup>, Daisuke ISHIHARA<sup>6</sup>, Hirokazu KATAZA<sup>1</sup>, Satoshi TAKITA<sup>1</sup>, Shinki OYABU<sup>6</sup>,  
Munetaka UENO<sup>1</sup>, Hideo MATSUHARA<sup>1</sup>, and Takashi ONAKA<sup>7</sup>

<sup>1</sup>*Institute of Space and Astronautical Science, Japan Aerospace Exploration Agency,  
3-1-1 Yoshinodai, Chuo-ku, Sagami-hara, Kanagawa 252-5210  
usui@ir.isas.jaxa.jp*

<sup>2</sup>*Okayama Astrophysical Observatory, National Astronomical Observatory, 3037-5 Honjo, Kamogata, Asakuchi, Okayama  
719-0232*

<sup>3</sup>*Max-Planck-Institut für Extraterrestrische Physik, Giessenbachstraße, 85748 Garching, Germany*

<sup>4</sup>*Department of Physics and Astronomy, Seoul National University, San 56-1, Shillim-dong Gwanak-gu, Seoul 151-742, South  
Korea*

<sup>5</sup>*Astronomical Institute, Tohoku University, 6-3 Aoba, Aramaki, Aoba-ku, Sendai 980-8578*

<sup>6</sup>*Graduate School of Science, Nagoya University, Furo-cho, Chikusa-ku, Nagoya, 464-8601*

<sup>7</sup>*Department of Astronomy, Graduate School of Science, The University of Tokyo, 7-3-1 Hongo, Bunkyo-ku, Tokyo 113-0033*

(Received 2011 February 10; accepted 2011 June 3)

## Abstract

We present the results of an unbiased asteroid survey in the mid-infrared wavelength with the Infrared Camera (IRC) onboard the Japanese infrared satellite AKARI. About 20% of the point source events recorded in the AKARI All-Sky Survey observations are not used for the IRC Point Source Catalog (IRC-PSC) in its production process because of the lack of multiple detection by position. Asteroids, which are moving objects on the celestial sphere, remain in these “residual events”. We identify asteroids out of the residual events by matching them with the positions of known asteroids. For the identified asteroids, we calculate the size and albedo based on the Standard Thermal Model. Finally we have a brand-new catalog of asteroids, named the Asteroid Catalog Using Akari (AcuA), which contains 5,120 objects, about twice as many as the IRAS asteroid catalog. The catalog objects comprise 4,953 main belt asteroids, 58 near Earth asteroids, and 109 Jovian Trojan asteroids. The catalog will be publicly available via the Internet.

**Key words:** infrared: solar system — minor planets, asteroids — space vehicles — catalogs — surveys

## 1. Introduction

The physical properties of asteroids are fundamental for the understanding of the formation process of our planetary system. In the present solar system, asteroids are thought to be the primary remnants of the original building blocks that formed the planets. They contain a record of the initial conditions of our solar nebula of 4.6 Gyr ago. The composition and size distribution of asteroids in the asteroid belt provide significant information on their evolution history, although they have experienced mutual collisions, mass depletion, mixing, and thermal differentiation, which have shaped their present-day physical and orbital properties.

The size and albedo are the basic physical properties of the asteroid. In some cases, combining the size and the mass that are measured precisely by the modern technique (Hilton 2002), the bulk density of the asteroid can be estimated (Britt et al. 2002). It is a powerful indicator to investigate the macroscopic porosity and the inner structure of the asteroid. The total mass and the size distribution of asteroids are crucial for the understanding of the history of the solar system (Bottke et al. 2005). The mineralogy and elemental composition of asteroids can also

be estimated from the albedo (Burbine et al. 2008).

There are several survey catalogs of asteroids: the 2MASS Asteroid Catalog (Sykes et al. 2000) compiles near-infrared colors of 1,054 asteroids based on the Two Micron All Sky Survey; the Subaru Main Belt Asteroid Survey (SMBAS; Yoshida & Nakamura 2007) gives the size and color distributions of 1,838 asteroids observed with the Subaru telescope; the SDSS Moving Object Catalog (SDSS MOC; Parker et al. 2008) consists of multi-color photometry of  $\sim 88,000$  asteroids from the Sloan Digital Sky Survey; the Sub-Kilometer Asteroid Diameter Survey (SKAD; Gladman et al. 2009) provides the size distribution of 1,087 asteroids based on observations with the 4-m Mayall telescope at Kitt Peak National Observatory. While these catalogs are based on optical to near-infrared observations, the size and albedo of asteroids are decoupled and can be determined solely independently, once mid-infrared observations are accomplished (Lebofsky & Spencer 1989; Bowell et al. 1989; Harris & Lagerros 2002).

Radiometric technique was first applied to determine the size and albedo of asteroids with ground-based observatories by Allen (1970) for 4 Vesta, Allen (1971) for 1 Ceres, 3 Juno, 4 Vesta, and Matson (1971) for 26 major main-belt asteroids. A pioneering systematic aster-

oid survey with a space-borne telescope was made by the Infrared Astronomical Satellite (IRAS) launched in 1983 (Neugebauer et al. 1984). IRAS observed more than 96% of the sky at the mid- and far-infrared 4 bands (12, 25, 60, and 100  $\mu\text{m}$ ) during the 10 month mission life. It derived the size and albedo of about 2,200 asteroids (Tedesco et al. 2002a). Another serendipitous survey was carried out by the Midcourse Space Experiment (MSX) launched in 1996 (Mill et al. 1994; Price et al. 2001). It observed  $\sim 10\%$  of the sky at 6 bands of 4.29, 4.35, 8.28, 12.13, 14.65, and 21.34  $\mu\text{m}$  and about 160 asteroids were identified, for which the size and albedo were provided (Tedesco et al. 2002b). Also the Infrared Space Observatory (ISO) launched in 1995 (Kessler 1996) made yet-another part-of-sky survey and observed several planets, satellites, comets, and asteroids at infrared wavelengths (Müller et al. 2002). Despite these extensive past surveys the asteroids for which the size and albedo have been determined are still only 0.5% of those with known orbital elements.

AKARI is the first Japanese space mission dedicated to infrared astronomy (Murakami et al. 2007). AKARI is equipped with a 68.5cm cooled telescope, a 170 liter superfluid liquid Helium (LHe), and two sets of two-stage Stirling cycle coolers. The focal plane instruments consist of the Infrared Camera (IRC) (Onaka et al. 2007) and the Far-Infrared Surveyor (FIS) (Kawada et al. 2007), each of which covers the spectral range of 2–26  $\mu\text{m}$  and 50–180  $\mu\text{m}$ , respectively. AKARI carried out the second generation infrared all-sky survey after IRAS. The All-Sky Survey is one of the main objectives of the AKARI mission in addition to pointed observations. It surveyed the whole sky at 6 bands in the mid- to far-infrared spectral range with the solar elongation angle of  $90 \pm 1$  degree to avoid the radiation from the Earth and the Sun. The AKARI satellite was launched on 2006 February 21 (UT). The All-Sky Survey had been continued until the LHe was boiled off on 2007 August 26. In total, more than 96% of the sky was observed with more than twice (Katata et al. 2010) during the cryogenic mission phase.

In this paper, we present a catalog of the size and geometric albedo of asteroids based on the IRC All-Sky Survey data. The IRC All-Sky Survey was carried out at two bands in the mid-infrared: *S9W* (6.7–11.6  $\mu\text{m}$ ) and *L18W* (13.9–25.6  $\mu\text{m}$ ). The IRC All-Sky Survey has advantages over the IRAS survey for detecting asteroids in the sensitivity and spatial resolution, both of which have been improved by an order of magnitude. The  $5\text{-}\sigma$  detection limit is 50 and 90 mJy at the *S9W* and *L18W* bands, respectively, and the spatial resolution of the IRC in the All-Sky Survey mode was about  $10''$  per pixel (Ishihara et al. 2010). Point source detection events are extracted and processed in the IRC All-Sky Survey observation data, from which the IRC Point Source Catalog (IRC-PSC, Ishihara et al. 2010) was produced by confirmation of the source with multiple detection in position. About 20% of the extracted events in the All-Sky Survey data are not used for the IRC-PSC because of the lack of confirmation detection. We identify asteroids out of the excluded events from the IRC-PSC. In this process,

we search for events whose positions agree with those of the asteroids with known orbits. The asteroid positions are calculated by the numerical integration of the orbit. We do not make an attempt to discover new asteroids in this project, whose orbital elements are not archived in the database. For each identified object, we calculate the size and albedo by using the Standard Thermal Model of asteroids (Lebofsky et al. 1986). Finally, we obtain an unbiased, homogeneous asteroid catalog, which contains 5,120 objects in total, twice as many as the IRAS asteroid catalog. This corresponds to about 1% of all the asteroids with known orbital elements.

This paper is organized as follows: In Sect.2, we describe the data reduction and the creation procedure of the asteroid catalog from the IRC All-Sky Survey data. In Sect.3, we describe the characteristics of the obtained catalog. In Sect.4, we summarize the paper and discuss the future prospect. Scientific output from this catalog will be discussed at length in a forthcoming paper (Usui et al. in preparation).

## 2. Data Processing and Catalog Creation

### 2.1. The AKARI IRC All-Sky Survey

The AKARI All-Sky Survey observation had started on 2006 April 24 as part of the performance verification of the instruments prior to the nominal observation, which started on 2006 May 8. In the All-Sky Survey observation mode, AKARI always points in the direction perpendicular to the Sun-Earth line on a sun-synchronous polar orbit, and rotates once every orbital revolution (see Fig.4 in Murakami et al. 2007). The telescope looks at the direction opposite to the Earth center to make continuous scans on the sky at a rate of  $216''\text{s}^{-1}$ . The orbital plane rotates around the axis of the Earth at the rate of the orbital motion of the Earth, and thus the whole sky can be observed in half a year. During the course of the AKARI LHe mission of 18 months, a given area of the sky was observed three or more times on average, depending on the ecliptic latitude. A large number of scan observations were made in the ecliptic polar regions, while only two scan observations (overlapping half of the FOV in contiguous scans) were possible in half a year for a given spot on the ecliptic plane. In this sense, solar system objects around the ecliptic plane have small observation opportunities with AKARI. In addition to the low visibility, other conditions further limit the observation opportunities near the ecliptic plane, including the disturbance due to the Moon and the South Atlantic Anomaly (SAA), latter of which is a high-density region of charged particles (mainly protons) at an altitude of a few hundred km above Brazil. Another complication was introduced to the operation after the first half year, which was called the offset survey. It was an “aggressive” operation to swing the scan path to complement imperfect scan observations in the first half year, which had been made in a “passive” survey mode. The first half year survey left many regions of the sky unobserved as gaps due to the Moon, the SAA, conflicts with pointed observations, and data downlink failures to the

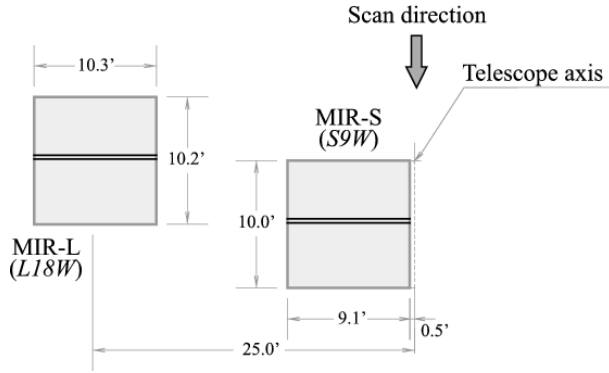


**Fig. 1.** Schematic view of the focal-plane layout of the IRC *S9W* (MIR-S) and *L18W* (MIR-L) detectors. Details are given in Murakami et al. (2007) and Onaka et al. (2007). The two solid lines in each detector denote the positions of the operating pixel rows (the 117th and 125th of the total 256 rows) for the All-Sky Survey observation mode. The separation between the two rows is exaggerated in this figure and in not in the real scale. Combining these two rows in the data processing, false signals due to cosmic ray hits are removed (milli-seconds confirmation, Ishihara et al. (2010)).

ground stations. To make up observations of these regions and increase the completeness of the sky coverage, the scan path was shifted from the nominal direction to fill the gaps on almost every orbit in the second and third half years (Doi et al. in preparation). For observations of solar system objects, the offset survey operation has both positive and negative effects. Some objects may lose the observation opportunities completely, while others may increase the number of detections drastically.

Since solar system objects have their orbital motions, the detection cannot be confirmed in principle by position on the celestial sphere. Moreover, *S9W* and *L18W* observe different sky regions of about 25' apart in the cross-scan direction because of the configuration on the focal plane (Fig.1) and an object is not observed with the 2 bands in the same scan orbit. Therefore, a single event of a point source needs to be examined without stacking for detection of asteroids.

Fig.2 shows the normalized spectral response function of *S9W* and *L18W*. The calculated model fluxes of asteroids are also shown.

In the following, we describe how asteroid events are extracted and identified in the All-Sky Survey observation and how their size and albedo are derived.

## 2.2. The Outline of Data Processing

The outline of the data processing to extract asteroid events is summarized in the following (see also Fig.3):

1. Point sources are extracted by the pipeline processing from the IRC All-Sky Survey image data. The extracted sources are matched in position with each other and those detected more than twice are regarded as confirmed sources and cataloged in the IRC-PSC. The detected sources not included in the IRC-PSC are considered to consist of extended

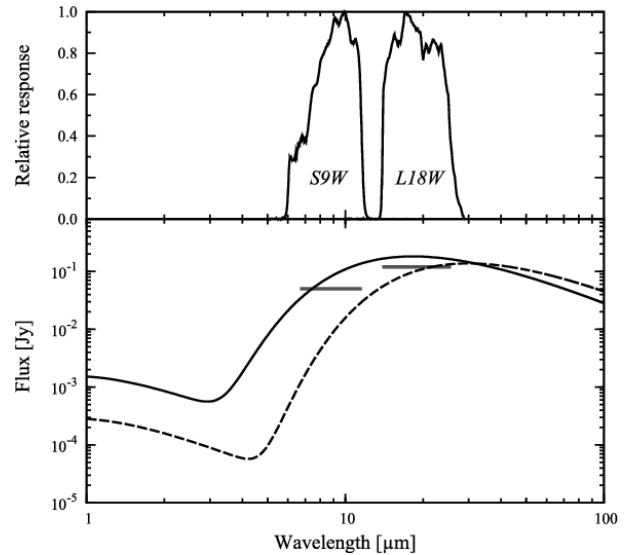


**Fig. 2.** Relative spectral response of *S9W* and *L18W* from [http://www.ir.isas.jaxa.jp/ASTRO-F/Observation/RSRF/IRC\\_FAD/](http://www.ir.isas.jaxa.jp/ASTRO-F/Observation/RSRF/IRC_FAD/) (upper panel). As reference, the model spectra of asteroids including the reflected sunlight and the thermal emission are shown in the lower panel. The solid line indicates the model flux of the asteroid with  $d = 5\text{km}$ ,  $p_v = 0.3$ ,  $R_h = 1.56\text{AU}$ , where  $d$ ,  $p_v$ , and  $R_h$  are the size (diameter), the geometric albedo, and the heliocentric distance, respectively. The Standard Thermal Model (Sect. 2.2.4) is used for the calculation. The dashed line indicates that with  $d = 33\text{km}$ ,  $p_v = 0.08$ ,  $R_h = 4.6\text{AU}$ . These two asteroids represent a lower limit in the size at the corresponding distance in the AKARI survey. The horizontal bars in the lower panel are also shown as the detection limits of *S9W* and *L18W*.

sources, signals due to high energy particles, geostationary satellites, and solar system objects as asteroids and comets (Sect.2.2.1). Hereafter, individual extracted point sources in the All-Sky Survey are called “events” and a summary of the events is called “event list”. The physical flux of each event is derived in the pipeline processing.

2. Identification of an event with an asteroid is carried out based on the predicted positions of the asteroids with known orbital elements (Sect.2.2.2).
3. Color corrections are applied to the fluxes of the events identified as asteroids, taking into account the heliocentric distance of the object. Events with large errors or those with very small fluxes are discarded from the list at this stage (Sect.2.2.3).
4. The size and albedo of each identified event are calculated based on the Standard Thermal Model (Sect.2.2.4).
5. Further screening of the sources is carried out and the final catalog is prepared (Sect.2.2.5).

### 2.2.1. Event list for asteroid identification

The present asteroid catalog is a secondary product of the IRC-PSC. Thus correction for detector anomalies, image reconstruction, point source extraction, pointing reconstruction, and flux calibration are applied in the same manner as in the IRC-PSC processing (Ishihara et al.

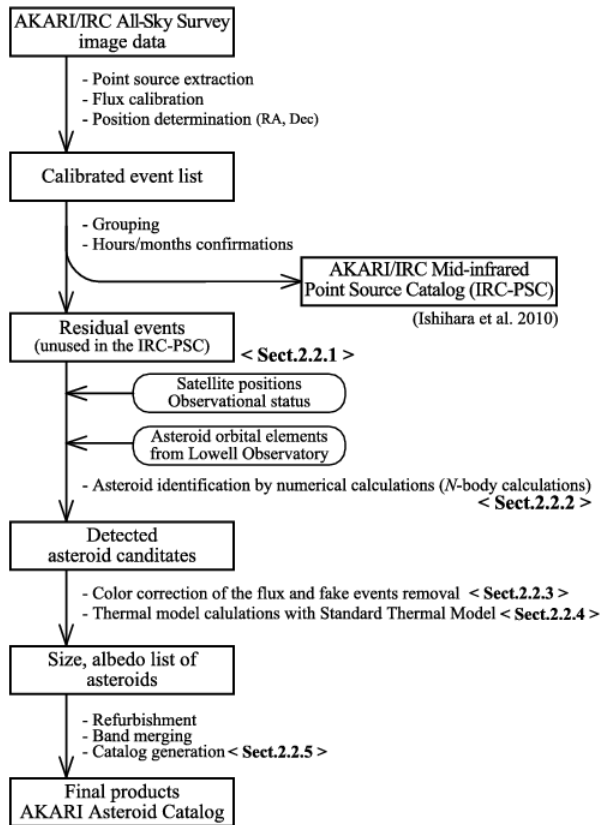


Fig. 3. Outline of the data processing to create the asteroid catalog.

2010). About 25% (*S9W*) and 18% (*L18W*) of the total events are not used for the IRC-PSC and they are analyzed in the present process (Table 1).

### 2.2.2. Asteroid identification

Identification with an asteroid is made based on the orbital calculation of the asteroids with known orbital elements.  $N$ -body simulations including gravitational perturbations with the Moon, eight planets, Ceres, Pallas, Vesta, and Pluto, are employed for the calculation. We regard the other asteroids as massless particles. The orbital elements of the asteroids are taken from the Asteroid Orbital Elements Database (Bowell et al. 1994) distributed at Lowell Observatory<sup>1</sup> at the epoch of 2010 04 14.0. It has 503,681 entries, which consist of 233,968 numbered and 269,713 unnumbered asteroids. Objects with large uncertainties in the orbital parameters, indicated as non-zero integers for the orbit computation in the database, are excluded. They include 19 numbered asteroids and 8,759 unnumbered. The positions of the Sun, planets, Moon, and Pluto are taken from DE405 JPL Planetary and Lunar Ephemerides in the J2000.0 equatorial coordinates at the NASA Jet Propulsion Laboratory. A Runge-Kutta-Nystrom 12(10) method (Dormand, El-Mikkawy, & Prince 1987) is used for the time integration with a variable time step.

The asteroid identification process is performed in the

following steps:

1. A 2-body (i.e., the Sun and a given asteroid) problem is solved at the epoch of the orbital elements of the asteroid to estimate the velocity and acceleration.
2. Given the observation time of an event detected with AKARI, the position of an asteroid is calculated back to that time by the  $N$ -body simulation. The integration time step is initially set as 1 day, and varied appropriately later in the following calculations. The calculated position is converted to the J2000.0 astrometric position (i.e., the position is revised with the correction for the light-time) since the positions of the events in the All-Sky Survey are given in the J2000.0 coordinates.

AKARI orbits in a sun-synchronous polar orbit at an altitude of 700km. The parallax between the geocenter and the spacecraft is not negligible particularly for Near Earth Asteroids, which amounts to an order of a few tens arcsec. Thus the apparent position relative to the AKARI spacecraft needs to be calculated. The spacecraft position is obtained by interpolation of the data from the AKARI observational scheduling tool, which has a sufficient accuracy for the present purpose.

3. The calculated positions are compared with those of the events detected in the All-Sky Survey. If the predicted position of an asteroid is located within  $2.5'$  from the position of an event, the process goes to the next step.
4. The apparent position of the asteroid is recalculated with a higher accuracy, taking account of the correction for the light-time, the gravitational deflection of light, the stellar aberration, and the precession and nutation of the Earth rotation. This process takes a large computation time and thus the calculation is made only for the events tentatively associated with an asteroid in the previous step.
5. The revised position of the asteroid and the position of the corresponding event are compared again. If the asteroid is located within  $7.5''$ , the position match is regarded as sufficient and the process goes to the next.
6. Then we check the predicted  $V$ -band magnitude ( $M_V$ ) of the asteroid at the observation epoch. If the predicted  $M_V$  is too faint, the asteroid should not have been detected with AKARI and the identification is regarded as false.  $M_V$  is calculated by using the formulation of Bowell et al. (1989) with the calculated heliocentric distance, “AKARI-centric” distance, the absolute magnitude ( $H$ ), and the slope parameter ( $G$ ). These  $H$ - $G$  values are taken from the dataset of Lowell Observatory as the same file as the orbital elements. These data mainly originate with the Minor Planet Center.

At the same time, the rate of change in the right ascension and declination seen from AKARI, the solar elongation and moon elongation angle, the phase

<sup>1</sup> The data available at <ftp://ftp.lowell.edu/pub/elgb/astorb.html>



**Table 1.** Number of the events for each processing step.

Event	<i>S9W</i>	<i>L18W</i>
(a) All events	4,762,074	1,244,249
(b) Events employed in the IRC-PSC	3,882,122	936,231
(c) Residual events	879,952	308,018
(d) Events identified as asteroids	6,924	13,760
(e) Asteroids in the final catalog	2,507	5,010
(f) Asteroids detected overall	5,120	

Notes:(a) “*Event*” indicates an individual detection of a point source in the All-Sky Survey data. (b) Events confirmed as a point source by multiple detection at the same celestial position (Ishihara et al. 2010). (c) Unused events in the IRC-PSC: (c) = (a) – (b). (d) Events identified as asteroids by the estimated positions. False identifications are excluded. (e) As is the column name. (f) Asteroids detected with either or both *S9W* and *L18W*.

angle (Sun-asteroid-AKARI angle), and the galactic latitude are calculated for later processes.

If the object is brighter than  $M_V < 23$ , the event is concluded to be associated as the asteroid. Otherwise the event is discarded.

It should be noted that that the 2.5' threshold of the position difference in step 3 is determined as the maximum value of the correction for the light-time assuming that a virtual asteroid with the moving speed of 11000 '/hr at 0.1 AU from the observer, as:

$$\frac{11000}{3600} ('/\text{sec}) \times 0.1(\text{AU}) \times 499.005(\text{sec}/\text{AU}) \sim 2.5' ,$$

and that the 7.5'' threshold in step 5 is determined as covering the signal shifted 1 pixel on the detector by chance where the pixel scale of the detector is 2.3'', the FWHM of the point source is 5.5'' (Kataza et al. 2010), and the position uncertainty including the corrections in step 4 is assumed less than 1'' .

### 2.2.3. Color correction and removal of spurious identification

Differences in color between the calibration stars used in the IRC-PSC (mainly K- and M-giants, Ishihara et al. 2010) and asteroids are not negligible because of the wide bandwidth of *S9W* and *L18W* and the continuum spectra in asteroids that cannot be assumed as perfect blackbody or graybodies. Therefore, we empirically approximate the color correction factors by a polynomial function of the heliocentric distance of the object as

$$F_{cc} = \frac{F_{\text{raw}}}{E_{\text{ccf}}} , \quad (1)$$

and

$$E_{\text{ccf}} = a_0 + a_1 R_h + a_2 R_h^2 + a_3 R_h^3 , \quad (2)$$

where  $F_{cc}$ ,  $F_{\text{raw}}$ ,  $E_{\text{ccf}}$  and  $R_h$  are the color corrected monochromatic flux at 9 or 18  $\mu\text{m}$ , the raw in-band flux, the color correction factor, and the heliocentric distance, respectively. This formula is evaluated using the predicted thermal flux and the relative spectral response functions of the *S9W* and *L18W* bands. The predicted thermal flux is calculated by assuming that a virtual asteroid with

**Table 2.** The coefficients of the color correction factors.

	$a_0$	$a_1$	$a_2$	$a_3$
<i>S9W</i>	0.984	-0.068	0.031	-0.0019
<i>L18W</i>	0.956	-0.024	0.007	-0.0003

$d = 100\text{km}$  and  $p_v = 0.1$  is located at a heliocentric distance between 1.0–6.0AU with a 0.05 AU step, where  $d$ , and  $p_v$  are the size (diameter), and the geometric albedo, respectively. We determine the coefficients  $a_0$ ,  $a_1$ ,  $a_2$ , and  $a_3$  as listed in Table 2. The fitting errors of equation (2) to the calculated model flux is 6% for *S9W* and 2.5% for *L18W* at most. The actual value of  $1/E_{\text{ccf}}$  is in a range of 1.06 – 0.80 for *S9W* and 1.07 – 0.99 for *L18W* for the heliocentric distance of 1–6 AU.

Up to this stage, the flux level of the event is not taken into account in the identification procedure. We discard false identifications in the following steps based on the flux level.

- Events with extremely large uncertainties in the flux are discarded. Here we set the threshold for the flux uncertainty as 71Jy for *S9W* and 96Jy for *L18W*. These threshold values are determined by a  $5\sigma$  clipping method, i.e., the standard deviation ( $\sigma$ ) of distribution of the flux uncertainties for all events is determined and the events of outside  $5\sigma$  values are discarded. 47 events at *S9W* and 101 events at *L18W* are discarded based on these criteria. This step in fact excludes events affected by the stray light near the Moon efficiently.
- The faintest sources in the IRC-PSC have fluxes of 0.045 Jy at *S9W* and 0.06 Jy at *L18W* (Ishihara et al. 2010). These values correspond to the signal-to-noise ratio ( $S/N$ ) of 6 and 3, respectively. There are a few events that have fluxes fainter than these values in the event list. Because of the low  $S/N$  of the fluxes, it is difficult to derive the size and albedo accurately for these objects. Thus these objects are also excluded from the catalog.

#### 2.2.4. Thermal model calculation

Radiometric analysis of the identified events is carried out with the calibrated, color corrected, monochromatic fluxes described in Sect.2.2.3. We used a modified version of the Standard Thermal Model (STM; Lebofsky et al. 1986). In the STM, it is assumed that an asteroid is a non-rotating, spherical body, and the thermal emission from the point on an asteroid's surface is in instantaneous equilibrium with the solar flux absorbed at that point. Then, the temperature distribution,  $T$ , on a smooth spherical surface of asteroid is simply assumed to be symmetric with respect to the subsolar point as:

$$T(\varphi) = \begin{cases} T_{\text{SS}} \cdot \cos^{1/4} \varphi, & \text{for } \varphi \leq \pi/2, \\ 0, & \text{for } \varphi > \pi/2, \end{cases} \quad (3)$$

where  $\varphi$  is the angular distance from the subsolar point. This assumes that the temperature on the nightside is treated as zero. The subsolar temperature,  $T_{\text{SS}}$ , is determined by equating the energy balance so that the absorbed sunlight is instantaneously re-emitted at thermal infrared wavelengths, thus,

$$T_{\text{SS}} = \left( \frac{(1 - A_b) S_s}{\eta \varepsilon \sigma R_h^2} \right)^{1/4}, \quad (4)$$

where  $A_b$ ,  $S_s$ ,  $\eta$ ,  $\varepsilon$ , and  $\sigma$  are the bond albedo, the incident solar flux, the beaming parameter, the infrared emissivity, and the Stefan-Boltzmann constant, respectively. It is usually assumed that

$$A_b = qp_v, \quad (5)$$

where  $q$ , and  $p_v$  are the phase integral, and the geometric albedo. The phase integral  $q$  is given (the standard H-G system; Bowell et al. 1989) by

$$q = 0.290 + 0.684G, \quad (6)$$

where  $G$  is the slope parameter.

The scattered light is observed at optical to near-infrared wavelengths. The diameter can then be derived from the relation as:

$$d = \frac{1329}{\sqrt{p_v}} 10^{-H/5}, \quad (7)$$

where  $d$ , and  $H$  are the diameter in units of km, and the absolute magnitude, respectively (see e.g., Fowler & Chillemi (1992)).

In applying the STM model, the parameters  $H$  and  $G$ , which are used in the identification process (Sect.2.2.2), are also employed as an optical flux. The infrared emissivity  $\varepsilon$  is assumed to be a constant of 0.9 as a standard value for the mid-infrared. The geometry is determined by the heliocentric distance, the AKARI-centric distance, and the phase angle. We assume a thermal infrared phase coefficient of 0.01 mag/deg as specified for the STM. For the error calculation we assign uncertainties of 0.05 mag for  $H$  and 0.02 for  $G$ . While the beaming parameter  $\eta$  basically accounts for the physical quantities relating to the surface roughness and the thermal inertia of the asteroid, it is used just as an empirical parameter, particularly in the STM.

The thermal flux of the model is calculated by integrating the Planck function numerically with equation (3) over a spherical asteroid of the diameter  $d$  under the condition of equation (7). The process is iteratively examined until the model flux converges on the observed value by adjusting the variables of  $d$  and  $p_v$ .

In the first analysis we concentrate on 55 selected, well-studied main-belt asteroids (Müller 2005), whose size, shape, rotational property, and albedo are known from different measurements (occultation, direct imaging, fly-bys, and radiometric techniques based on large thermal datasets) as listed in Table 11 in Appendix 2. These samples include asteroids of the sizes between about 70 and 1000 km and the albedos from 0.03 to 0.4. The verification of the STM approach for a given AKARI asteroid is examined with this dataset. Lebofsky et al. (1986) made a similar exercise for 1 Ceres and 2 Pallas and derived a beaming parameter of  $\eta = 0.756$  to obtain an acceptable match between the radiometrically derived size and albedo from  $N$ - and  $Q$ -band fluxes of ground-based observations and the published occultation diameters. For the AKARI dataset of  $S9W$  and  $L18W$ , we adjust the beaming parameter to obtain the best fit in the size and albedo between the values derived from the AKARI 2-band data and the known values. The best fit is obtained with  $\eta = 0.87$  for  $S9W$  and 0.77 for  $L18W$ . We also attempt to fit the 2-band data simultaneously with a single  $\eta$  for the objects for which both data are available at the same epoch. However the overall match becomes significantly worse. We therefore decided to use different values of  $\eta$  for each band.

#### 2.2.5. Final adjustment and creation of the catalog

Thermal model calculations provide unreasonable values (either too bright or too dark) for some asteroids. They are regarded as false identification. We set the threshold for albedo as  $0.01 < p_v < 0.9$  and those outside of the range are discarded. The number of the discarded events at this stage is 178 for  $S9W$  and 53 for  $L18W$ , about 1 % of the total identified events.

To obtain the final product, we take a mean of the size and albedo with the weight of the  $S/N$  for each object. For the IRC All-Sky Survey data, the  $S/N$  is given as a function of the measured flux (see Fig.15 in Ishihara et al. 2010). For the asteroids, about 68% of  $S9W$  and 74% of  $L18W$  events reach the maximum  $S/N$  values,  $S/N = 15$  for  $S9W$  and  $S/N = 18$  for  $L18W$ . The corresponding flux is about 0.6Jy at  $S9W$  and 1.0Jy at  $L18W$ . If all the fluxes of an asteroid are above these values, the weighted mean is equal to a simple arithmetic mean.

Finally, a total of 5,120 objects (5,079 numbered, and 41 unnumbered asteroids) are included in the catalog of the AKARI Mid-infrared Asteroid Survey, named the Asteroid Catalog Using Akari (AcuA).

### 3. Evaluation of the asteroid catalog

#### 3.1. Uncertainty of the catalog data

One of the most major contributions which bring uncertainties in the size and albedo is the uncertainty of the

observed fluxes of the asteroids. It is expressed in terms of the  $S/N$  of the fluxes of the events in the IRC-PSC. As mentioned in Sect.2.2.5, the  $S/N$  have reached a plateau at  $S/N = 15$  for  $S9W$  and  $S/N = 18$  for  $L18W$ . Thus even for the best cases the uncertainties in the fluxes are 6.7% and 5.6%, for  $S9W$  and  $L18W$ , respectively. This is directly result in uncertainties in the size of 3.3% and 2.8% and in the albedo of 6.7% and 5.6%. It is inherent component in this work.

The absolute magnitude ( $H$ ) is adopted from the same dataset of Lowell Observatory as for the orbital elements described in Sect.2.2.2. The uncertainty in  $H$  is given as three levels: 0.5, 0.05, and 0.005mag in the dataset. We suspect that the visual absolute magnitude  $H$  has a large uncertainty and probably larger than those cataloged in some cases. Thus we decided to give a constant uncertainty of 0.05 mag for objects listed with the uncertainties of 0.005mag (963 asteroids) and 0.05 mag (4,157 asteroids) of our 5,210 cataloged asteroids rather than to use the original uncertainties in the dataset. This corresponds to a 4.6% uncertainty in albedo and less in size. The slope parameter ( $G$ ) is also taken from the dataset of Lowell Observatory. In our cataloged asteroids, 5,015 objects are assumed as  $G = 0.15$  and others are provided severally. The uncertainty of  $G$  is assumed as 0.02 uniformly. It has a small influence on the derived size and albedo as expected in equation (6).

In our catalog, these three parameters, i.e., the observed fluxes, the absolute magnitude  $H$ , and the slope parameter  $G$  are considered as the contributed factors for the uncertainties in the size and albedo. From these combination, typical values of uncertainties in size is 4.7%, and those in albedo is 10.1%. The other components discussed below are not used for the uncertainty calculation because they are not appropriately quantified in this work.

In this work, we apply the STM (Sect.2.2.4) to derive the size and albedo. It is assumed that an asteroid is a non-rotating, spherical body at a limit of zero thermal inertia. Thus the flux variation due to rotation of an object is neglected. Detailed investigations require further information on the object, such as the individual shape model, the direction of the spin vector, and so on. Since continuous observations with AKARI have at least a 100 minute interval (one orbital period of the satellite) inevitably, light curves with fine time resolution cannot be obtained. Therefore it is difficult to determine the detailed model parameters solely by AKARI observations. It is known that many asteroids have large amplitude ( $\sim$  a few tens %) in the light curves (Warner et al. 2009). This adds a few to  $\sim 10\%$  uncertainties in size, especially for those with a small number of detections. Therefore the uncertainties in the size and albedo originating from the flux uncertainty could be larger for those asteroids.

The model parameters in the STM are the emissivity ( $\epsilon$ ), the thermal infrared phase coefficient, and the beaming parameter ( $\eta$ ). The former two are given as fixed values in advance. Because of a severe constraint on the solar elongation angle, observations with AKARI cannot be made with several different phase angles. For this rea-

son, the phase coefficient is fixed as 0.01mag/deg in the present analysis (Matson 1971). The different values are used for the beaming parameter  $\eta$  for  $S9W$  and  $L18W$ . The different values are chosen to adjust the derived size and albedo to those reported in previous work. The failure of any single value of  $\eta$  to provide good results with previous work may stem from the invalid assumptions in the STM. The beaming parameter is in fact not a physical quantity, but rather introduced to account for the observations empirically. AKARI did not observe an asteroid with the two bands simultaneously, which could affect the way of the adjustment of  $\eta$  at the two bands. The uncertainty of  $\eta$ , a 5% change in  $\eta$  leads to about 4% and 2% changes in size and about 8% and 5% changes in albedo at  $S9W$  and  $L18W$ , respectively, depending slightly on the albedo of the object.

The geometry is given by the heliocentric distance, the AKARI-centric distance, and the phase angle. These are dependent on the position accuracy of the IRC-PSC (less than  $2''$ , Ishihara et al. (2010)), and their uncertainties are negligible for the obtained catalog values.

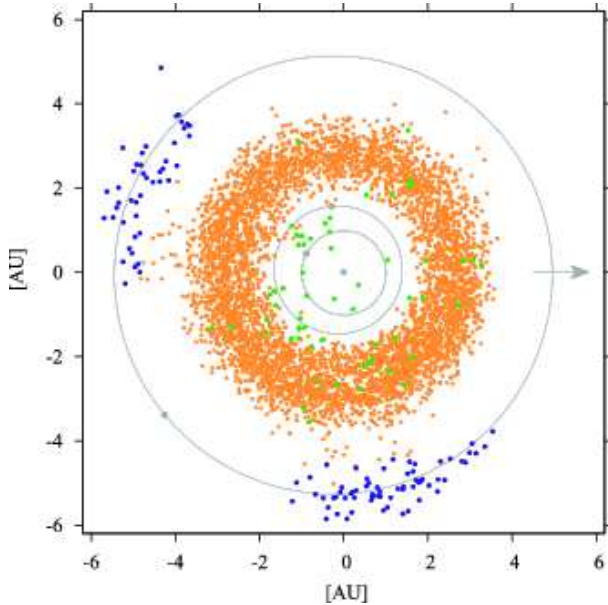
### 3.2. Total number and spatial distribution

The number of the asteroids identified in the AKARI All-Sky Survey is summarized in Table 1. The net number of the asteroids detected with  $S9W$  and  $L18W$  in total is 5,120. The number of the asteroids detected at  $L18W$  is by about twice larger than that at  $S9W$ . The number of the point sources detected at  $S9W$  in the IRC-PSC is approximately four times as many as that at  $L18W$ . The opposite trend can be explained by the different spectral energy distribution of the objects: asteroids have typical effective temperatures around 200K and radiate thermal emission with the peak wavelength of  $\sim 15 \mu\text{m}$ , which can preferentially be detected at  $L18W$  even if the difference in the sensitivity is taken account (Fig.2). Stellar sources emit radiation with the peak wavelength at UV to optical and thus are detected with higher probabilities at  $S9W$ . A significant fraction of asteroids, particularly in the main-belt rather than the near-Earth, is detected only at  $L18W$ , but undetected at  $S9W$  because of the steep decrease in the thermal radiation in the Wien's domain.

In Fig.4, we show the distribution of the identified asteroids projected on the ecliptic plane (i.e., the face-on view). The near Earth asteroids (NEAs), the main-belt asteroids (MBAs), and the Jovian Trojans can be discerned in the plot, while Centaurs and Trans-Neptune objects are not detected in our survey. Fig.4 displays the location of the 5,120 asteroids at the epoch of 2006 February 22. It shows the distribution of asteroids without any bias and survey gap.

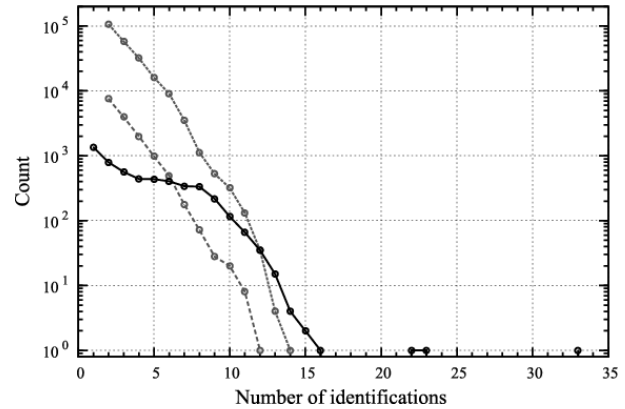
### 3.3. Number of detections per asteroid

Fig.5 illustrates the number of detections for each asteroid with the AKARI All-Sky Survey. For comparison, we also plot the number of detections for the point sources in the IRC-PSC around the ecliptic plane, which includes galactic and extragalactic objects. AKARI basically observes a given portion of the sky at least twice in con-



**Fig. 4.** Distribution of the identified asteroids projected on the ecliptic plane as of 2006 February 22. The circles indicate the orbits of the Earth, Mars, and Jupiter from inside to outside. The orange, green, and blue dots indicate the MBAs, the NEAs, and the Trojans, respectively. The arrow shows the direction of the vernal equinox.

tiguous scans. Hence, a point source should have been observed four times at  $S9W$  and  $L18W$  in total. Because the lifetime of the AKARI cryogenic mission phase was 550 days, it observed a given portion of the sky in three different seasons. Accordingly AKARI should have observed a point source on the ecliptic plane 12 times on average. The number could decrease because of the disturbance due to the SAA and the Moon or increase by the offset survey described in Sect.2.1. For the solar system objects, the situation is complicated due to their orbital motions. Considering the rate of change in the ecliptic longitude ( $d\lambda/dt$ ), there are only five objects in AKARI catalog of  $1.8'/\text{hr} < d\lambda/dt < 4.0'/\text{hr}$ : 137805 ( $2.96'/\text{hr}$ ), P/2006 HR30 ( $3.50'/\text{hr}$ ), 85709 ( $2.95'/\text{hr}$ ), 7096 Napier ( $1.93'/\text{hr}$ ), and 7977 ( $2.66'/\text{hr}$ ), while the scan path of the All-Sky Survey shifts at most by  $\sim 2.47'/\text{hr}$  ( $= 360^\circ/\text{yr}$ ) in the ecliptic longitude (i.e., in the cross-scan direction). The orbits of these objects are illustrated in Fig.6. These objects except for 7977 have a large number of detections, e.g., more than 15 times, suggesting that they keep up with the scan direction: 33 times for 137805, 23 times for P/2006 HR30, 22 times for 85709, and 15 times for 7096 Napier. Although P/2006 HR30 is classified as a Halley-type comet (the Tisserand invariant value of  $T_J = 1.785$ ; Hicks & Bauer (2007)) and its cometary activity is reported (Lowry et al. 2006), we include this object as an asteroid in this paper. 7977 has only 3 detections at  $S9W$ , due to the interference with pointed observations as well as to the "negative" effect of the offset survey. 366 has  $d\lambda/dt = 0.49'/\text{hr}$ , which is out of the range of the "keep up" speed mentioned above, but it was observed 16 times.



**Fig. 5.** Histogram of the number of detections of the asteroids identified with the AKARI All-Sky Survey (solid line). The objects with extremely large numbers are 137805 (1999 YK5) with 33, P/2006 HR30 (Siding Spring) with 23, 85709 (1998 SG36) with 22, and 366 Vincentina (1893 W) with 16 detections. The gray dashed and the gray dotted lines show the number of the events with the sum of  $S9W$  and  $L18W$ , which are used as input to the IRC-PSC (Kataza et al. 2010), for  $|\beta| < 1^\circ$  and  $|\beta| < 15^\circ$ , respectively, where  $\beta$  is the ecliptic latitude of the source.

It has three observation opportunities and at one of them (2006/11) the number of detections was increased by the "positive" effect of the offset survey.

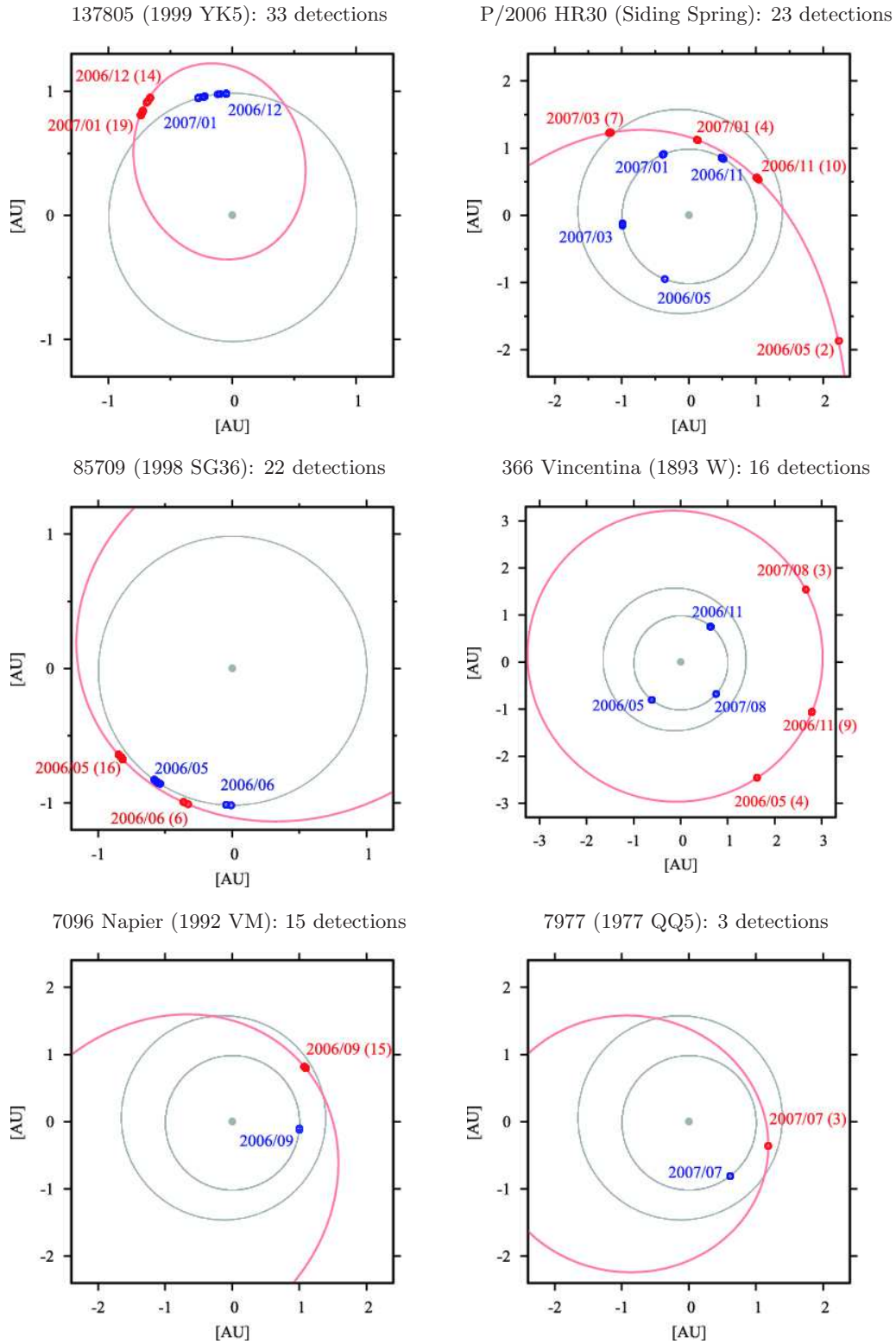
The present catalog contains only asteroids with the prograde motion with the Earth and no asteroids with the retrograde motion are included. The sources with multiple detection are more reliable in terms of the confirmation in general. The IRC-PSC only includes objects that are detected at the same position at least twice. The present catalog has 5,120 asteroids with  $N_{ID} \geq 1$ , and 3,771 asteroids with  $N_{ID} \geq 2$ , where  $N_{ID}$  is the number of the events with  $S9W$  and  $L18W$  in total. It should be noted that the catalog includes asteroids with single detection ( $N_{ID} = 1$ ). The number of the detection is listed in the catalog (Appendix 1).

### 3.4. Size and Albedo distribution

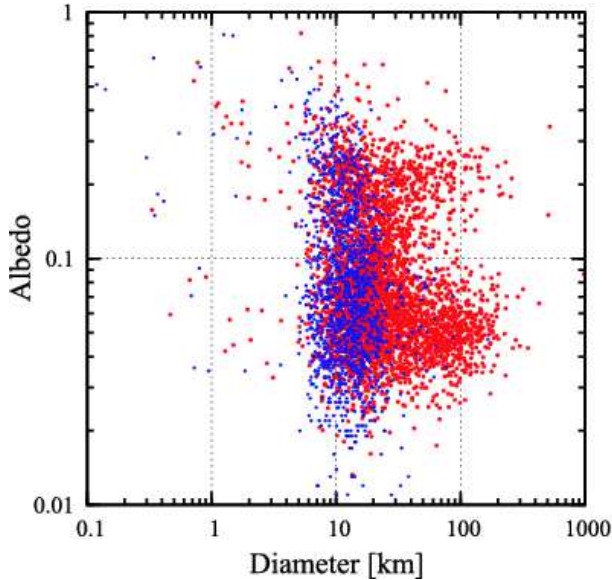
Fig.7 shows the distribution of albedos as a function of diameter for the asteroids detected with the AKARI All-Sky Survey. An outstanding feature is the bimodal distribution in the albedo. It is also suggested that the albedo increases as the size decreases for small asteroids ( $d < 5\text{km}$ ), although the number of the asteroids with the size of  $d < 5\text{km}$  is not large. In the catalog, the smallest asteroid is 2006 LD1, whose size is  $d = 0.12 \pm 0.01\text{km}$ . The largest one is, naturally, 1 Ceres of  $d = 970 \pm 13\text{km}$ .

Fig.8 illustrates the histograms of the asteroids detected with the AKARI All-Sky Survey as a function of the size and the albedo. For comparison, the results of IRAS observations are also plotted. The IRAS catalog consists of 2,228 objects with multiple detections and 242 objects with single detection (at  $12\mu\text{m}$  band). It clearly indicates that the AKARI All-Sky Survey is more sensitive to small asteroids than IRAS. Concerning about the size distribution of asteroids, the number is supposed to in-





**Fig. 6.** Orbits of the asteroids with the large number of detections projected on the ecliptic plane. 7977 is an exceptional case in this figure (only 3 detections; see text). The red and blue open circles indicate the positions of the asteroids as of their detections, and those of the Earth, respectively. The number of detections are given in the parentheses following the year/month of the observations. The orientation is the same as Fig.4 but the scale is different.



**Fig. 7.** Distribution of the size (diameter) and albedo of all the 5,120 identified asteroids. Red dots show those with more than two events and blue ones indicate those with single event detection.

crease monotonically as the decrease of the size. Fig.8(a), however, shows maxima around  $d = 15\text{km}$  for AKARI and  $30\text{km}$  for IRAS. The profiles of the histogram are similar to each other for those larger than  $30\text{km}$ , suggesting that IRAS and AKARI exhaustively detect asteroids of the size  $d > 30\text{km}$  and  $d > 15\text{km}$ , respectively, but that the completeness rapidly drops for asteroids smaller than these values. We discuss further on the size distribution in the following section. Fig.8(b) clearly indicates that the albedo of the asteroids has the well known bimodal distribution (Morrison 1977b). The bimodal distribution can be attributed to two groups of taxonomic types of the asteroids. The primary peak around  $p_v = 0.06$  is associated with C- and other low albedo types and the secondary peak around  $p_v = 0.2$  with S- and other types with moderate albedo. Further discussion concerning about the taxonomic types will be discussed in a forthcoming paper (Usui et al. in preparation).

### 3.5. V-band magnitude of the identified asteroids

Fig.9 shows the calculated V-band magnitude ( $M_V$ ) against the color-corrected monochromatic flux of the events identified as asteroids. 3,771 asteroids have multiple events in the AKARI All-Sky Survey. For example, 4 Vesta is observed with the flux of 134–139 Jy at S9W (2 times) and 474–604 Jy at L18W (3 times) with  $M_V = 7.3$ , 1 Ceres is observed with the flux of 127–142 Jy at S9W (3 times) and 497–853 Jy at L18W (4 times) with  $M_V = 8.9 - 9.0$ , and 7 Iris is observed with the flux of 37–96 Jy at S9W (3 times) and 238–254 Jy at L18W (4 times) with  $M_V = 9.3 - 9.4$ . The bimodal characteristic is also seen in Fig.9. A sharp cutoff of the flux at below  $\sim 0.1\text{Jy}$  is the result of the rejection of faint objects in the catalog processing (Sect.2.2.3).

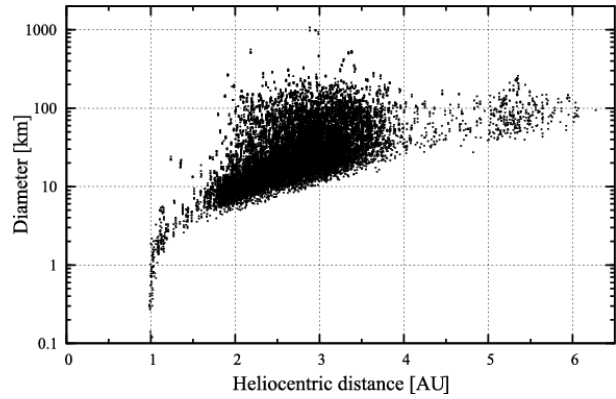


**Fig. 10.** Distribution of the estimated size (diameter) vs. the heliocentric distance for the detected asteroids at the epoch of the observation with AKARI.

We set a threshold for  $M_V$  in the identification process (in step 7 in Sect.2.2.2). The objects of the faintest  $M_V$  in Fig.9 are 67999 (2000 XC32) with  $M_V = 19.8$  at S9W and 102136 (1999 RO182) with  $M_V = 20.3$  at L18W. It should be noted that both objects are observed only once in the AKARI All-Sky Survey. This result confirms that the threshold of  $M_V = 23$  in Sect.2.2.2 is reasonable to select real asteroids.

### 3.6. Detection limit of the size of asteroids

Fig.10 shows the estimated size of the asteroids as a function of the heliocentric distance at the epoch of AKARI observation. It is reasonable that smaller asteroids are detected more in near-Earth orbits. No asteroids are detected inside of the Earth orbit because the viewing direction of the AKARI is fixed at the solar elongation of  $90 \pm 1$  degree. The smallest asteroids detected around the Earth orbit, the outer main-belt ( $3.27\text{AU}$ ), and Jupiter's orbit ( $5.2\text{AU}$ , Trojans) are  $0.1\text{km}$ ,  $15\text{km}$ , and  $40\text{km}$ , respectively.

### 3.7. Possibility of discovery of new asteroids

In the asteroid catalog processing, we did not take into account detection of new asteroids whose orbital parameters are not known. Reliable detection of unknown moving objects require a high redundancy in the observation, which the AKARI All-Sky Survey did not provide. Unfortunately the low visibility for observations around the ecliptic plane makes it difficult to reliably detect new asteroids solely from the AKARI All-Sky Survey database. However it is also very likely that the AKARI All-Sky Survey database contains signals of undiscovered asteroids. In fact, we belatedly found that some asteroids had been detected with AKARI before their discovery. For instance, 2006 SA6, which was discovered on 2006 September 16 (Christensen et al. 2006), had been detected on 2006 June 25 with AKARI, and 2007 FM3, which was discovered on 2007 March 19 (Kowalski et al. 2007), had been observed on 2007 February 16 with AKARI (discovery of these two were done by Catalina Sky Survey). Thus whenever a new asteroid is discovered, we could check the

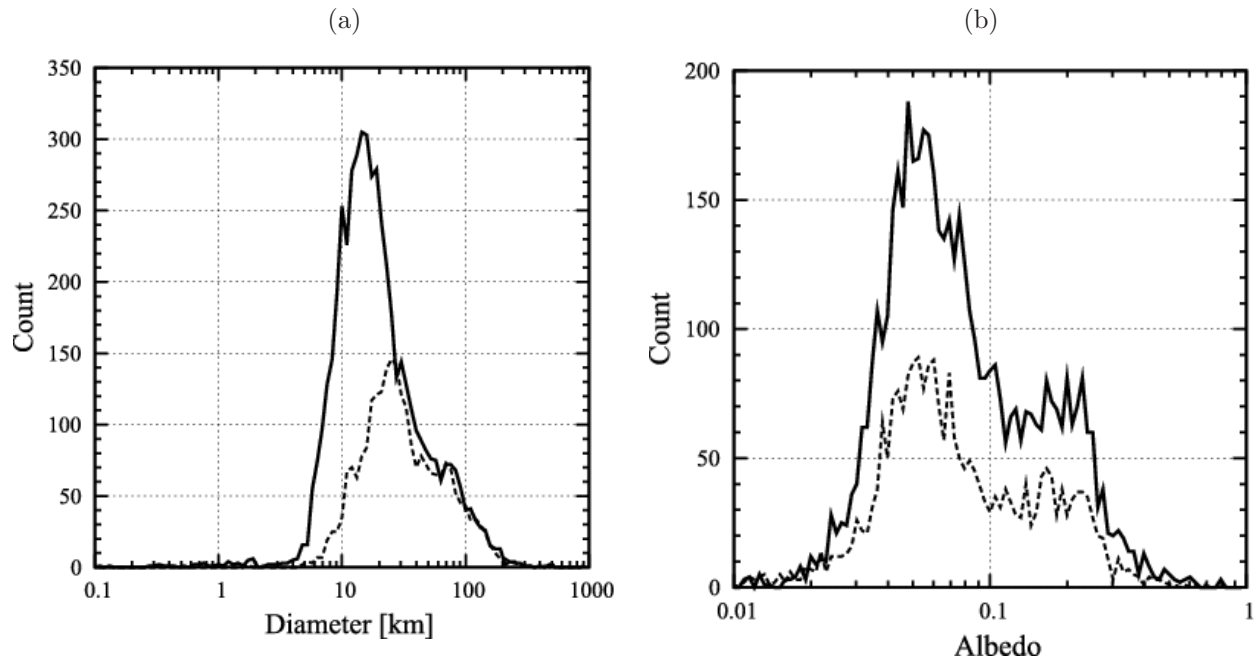


Fig. 8. Histograms of (a) the size (diameter) and (b) the albedo. The solid, and dashed lines indicate the results from AKARI, and IRAS observations (Tedesco et al. 2002a), respectively. The bin size is set as 100 segments for the range of 0.1km to 1000km in the logarithmic scale for (a) and 100 segments for the range of 0.01 to 1.0 in the logarithmic scale for (b).

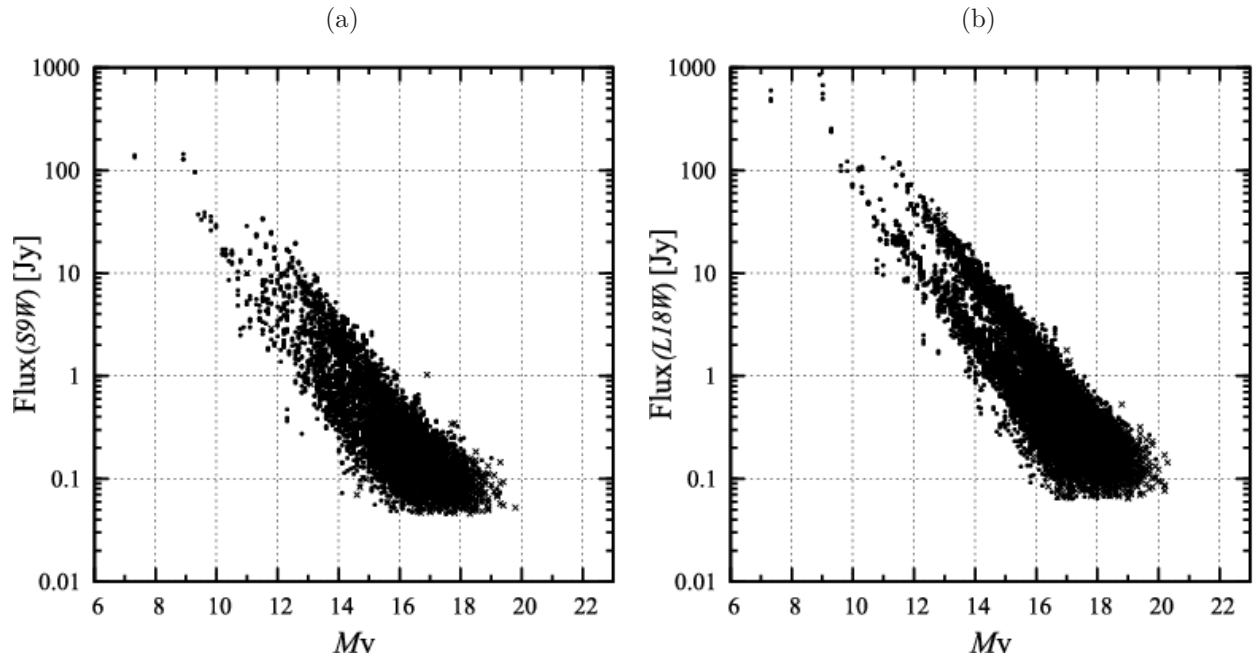
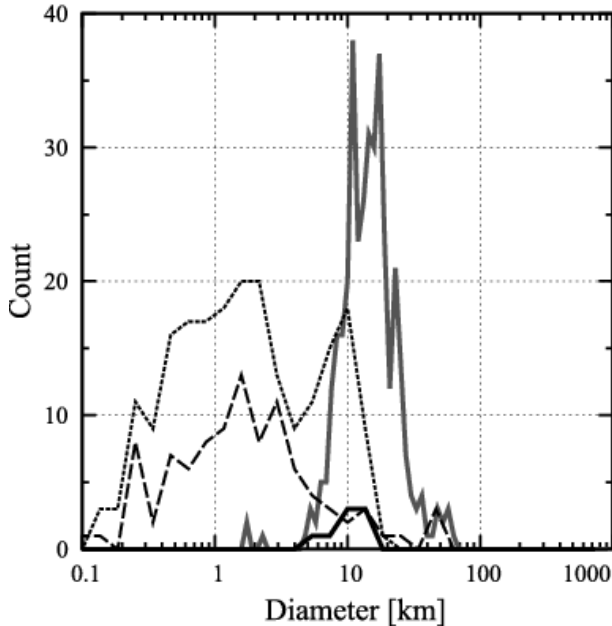
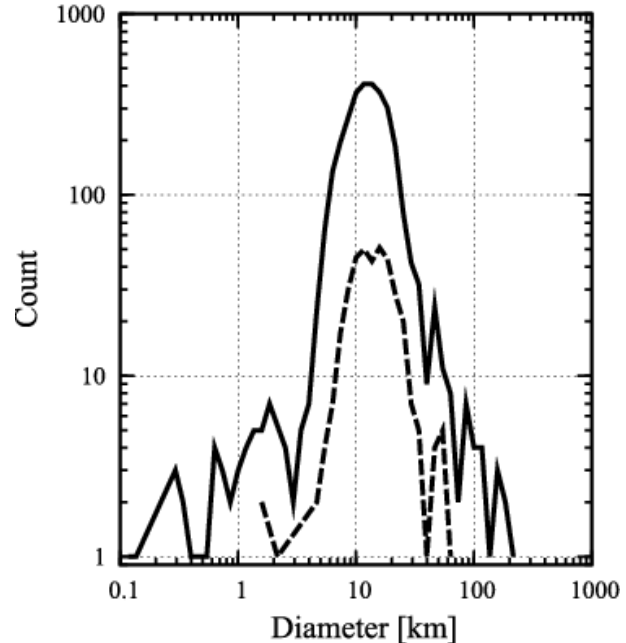


Fig. 9. Calculated  $V$ -magnitude ( $M_V$ ) vs. color-corrected (monochromatic) flux of the events identified as asteroids at S9W and L18W.



**Fig. 11.** Histogram of the asteroids with the previously determined size (diameter) without AKARI observations. The gray solid, black solid, black dotted, and black dashed lines indicate the data with IRAS, MSX, SST, and other observatories, respectively. The references are summarized in Appendix 3. The bin size is set as 30 segments for the range of 0.1km to 1000km in the logarithmic scale except for the data with IRAS, for which the bin size is set as 100 segments.



**Fig. 12.** Histogram of the size (diameter) of the asteroids determined either by AKARI or IRAS observations. The solid and dashed lines indicate the numbers of the asteroids that are detected with AKARI but undetected with IRAS, and vice versa, respectively. The bin size is set as 60 segments for the range of 0.1km to 1000km in the logarithmic scale.

detection in the AKARI All-Sky Survey database.

### 3.8. Comparison with previous work

#### 3.8.1. Total number of detections

The total numbers of the detected asteroids with AKARI and previous work are summarized in Table 3. The detected asteroids with AKARI are about twice as many as that of IRAS. A few hundreds of asteroids are not detected with AKARI, which have been observed previously. Fig.11 shows the size distribution of the asteroids undetected with AKARI. Most observations of these asteroids were made with the Spitzer Space Telescope (SST) and ground-based telescopes in programs to detect small asteroids. Fig.11 indicates that AKARI All-Sky Survey did not detect hundreds of small asteroids of  $d < 15$ km due the sensitivity limit.

#### 3.8.2. Comparison with IRAS

Fig.12 shows the histogram of the asteroids detected with AKARI without IRAS detection. A clear peak appears around the size of  $d \sim 15$ km, indicating that the AKARI All-Sky Survey extends the asteroid database down to  $d \sim 15$ km. Table 4 shows large ( $d > 100$ km) asteroids detected with AKARI but undetected with IRAS. Out of fifteen asteroids in this list, the size and albedo of three asteroids (375 Ursula (1893 AL), 190 Ismene, and 275 Sappientia) have been determined by our measurements for the first time. The size and albedo of the other twelve asteroids have been estimated with ground-based and space-borne telescopes previously. The AKARI aster-

oid catalog does not contain several very large ( $d > 40$ km) asteroids detected with IRAS (Table 5). For these asteroids, the size information is derived from IRAS observations. All of these asteroids are distant objects and belong to the Jovian Trojans except for 3 Hildas: 11542 (1992 SU21), 4317 Garibaldi (1980 DA1), and 13035 (1989 UA6). The semi-major axes of these objects are larger than 3.9 AU. The closest heliocentric distances are about 5.1AU for the Trojans and 4.4AU for the Hildas at the time of the AKARI All-Sky Survey observation.

The largest asteroid that AKARI failed to detect is 22180 (2000 YZ), whose size is  $d = 64$ km according to IRAS observations. We examine the original scan data for these undetected large asteroids and confirm that two asteroids, 22180 (2000 YZ) and 4317 (1980 DA1), can be seen in raw images of the All-Sky Survey data at  $L18W$  only once. They are, however, rejected because they are detected near the edge of the detector. The other two asteroids, 14268 (2000 AK156) and 11542 (1992 SU21), are confused with stellar objects since they are located at galactic latitudes less than 1 degree at the epoch of the observation. For the other asteroids, no particular reasons for non-detection are found. Some of them may lose the observation opportunities due to the offset survey operation mentioned in Sect.2.1. Deformed shapes, if any, may account for the non-detection with AKARI.

Fig.13 shows a comparison of the size and the albedo estimated from AKARI and IRAS observations for 2,221 asteroids (Table 6). The two measurements show fairly good agreement. The correlation coefficients are 0.9895



**Table 3.** Number of asteroids with derived radiometric size/albedo information. AKARI catalog compared to IRAS (Tedesco et al. 2002a), MSX (Tedesco et al. 2002b), SST (summarized in Appendix 3:C1–C10), and other observations (in Appendix 3:D1–D67).

	AKARI	IRAS	MSX	SST	others
asteroids with AKARI observations	5,120	2,103	160	7	288
asteroids without AKARI observations	—	367	8	211	97
total	5,120	2,470	168	218	385

**Table 4.** List of the asteroids that are detected with AKARI but undetected with IRAS ( $d > 100\text{km}$ , 15 objects). The parameters  $d$ ,  $p_v$ ,  $a$ ,  $e$ , and  $i$  indicate the size (diameter), the albedo, the semi-major axis, the eccentricity, and the inclination of the asteroids, respectively. The references are summarized in Appendix 3. The cited data refer to the underlined reference in the list. For those with the asterisks, namely, 375 Ursula, 190 Ismene, and 275 Sapienia, the AKARI data provide the first determination of the size and albedo.

Asteroid	orbital elements			AKARI		previous work		
	$a$ [AU]	$e$	$i$ [deg]	$d$ [km]	$p_v$	$d$ [km]	$p_v$	References
624 Hektor 1907 XM	5.23749517	0.02237543	18.181769	$230.99 \pm 3.94$	$0.034 \pm 0.001$	239.20	0.041	<u>D45</u> , D58
19 Fortuna	2.44236038	0.15765176	1.572523	$199.66 \pm 3.02$	$0.063 \pm 0.002$	201.70	0.064	D3, D5, D7, D16, <u>D55</u>
375 Ursula 1893 AL	3.12268315	0.10721155	15.949598	$193.63 \pm 2.52$	$0.049 \pm 0.001$	—	—	(*)
190 Ismene	3.98157898	0.16462886	6.166222	$179.89 \pm 3.64$	$0.051 \pm 0.003$	—	—	(*)
24 Themis	3.12872103	0.13118619	0.759515	$176.81 \pm 2.30$	$0.084 \pm 0.003$	176.20	0.084	D52, <u>D55</u>
9 Metis	2.38647903	0.12228869	5.574494	$166.48 \pm 2.08$	$0.213 \pm 0.007$	154.67	0.228	<u>B1</u> , D3, D5, D42, D52, D55
14 Irene	2.58571736	0.16721133	9.105428	$144.09 \pm 1.94$	$0.257 \pm 0.009$	155.00	0.170	<u>D3</u> , D5
884 Priamus 1917 CQ	5.16616811	0.12330089	8.925189	$119.99 \pm 2.13$	$0.037 \pm 0.001$	138.00	0.034	<u>D45</u>
129 Antigone	2.86777878	0.21205688	12.218688	$119.55 \pm 1.42$	$0.185 \pm 0.005$	115.00	0.187	<u>D7</u>
275 Sapienia	2.77846168	0.16053249	4.768788	$118.86 \pm 1.76$	$0.036 \pm 0.001$	—	—	(*)
3451 Mentor 1984 HA1	5.10303310	0.07129302	24.695344	$117.91 \pm 3.19$	$0.075 \pm 0.005$	122.20	0.052	<u>D45</u>
127 Johanna	2.75462967	0.06479782	8.241708	$114.19 \pm 1.52$	$0.065 \pm 0.002$	123.33	0.056	<u>B1</u>
27 Euterpe	2.34596656	0.17303724	1.583754	$109.79 \pm 1.54$	$0.234 \pm 0.008$	118.00	0.110	<u>D3</u> , D5
481 Erita 1902 HP	2.74051861	0.15484764	9.837640	$103.53 \pm 1.90$	$0.061 \pm 0.003$	113.23	0.050	<u>B1</u>
505 Cava 1902 LL	2.68527271	0.24493942	9.839062	$100.55 \pm 1.24$	$0.063 \pm 0.002$	115.80	0.040	<u>D55</u>

**Table 5.** List of the asteroids which are detected with IRAS, not with AKARI ( $d > 40\text{km}$ , 11 objects). The columns are the same as in Table 4.

Asteroid	orbital elements			previous work			
	$a$ [AU]	$e$	$i$ [deg]	$d$ [km]	$p_v$	References	
22180	2000 YZ	5.19497082	0.07172030	29.276964	64.18	0.052	<u>A1</u>
18137	2000 OU30	5.13890227	0.01629281	7.655306	60.71	0.013	<u>A1</u>
5027	Androgeos 1988 BX1	5.30195674	0.06662613	31.450673	57.86	0.092	<u>A1</u>
5025	1986 TS6	5.20547347	0.07670562	11.022628	57.83	0.064	<u>A1</u>
14268	2000 AK156	5.26980857	0.09197994	14.950850	57.54	0.037	<u>A1</u>
6545	1986 TR6	5.12777404	0.05220160	11.998200	56.96	0.055	<u>A1</u>
11542	1992 SU21	3.95030034	0.24086237	6.876531	49.72	0.022	<u>A1</u>
4317	Garibaldi 1980 DA1	3.98754535	0.16071342	9.823735	49.50	0.050	<u>A1</u>
13362	1998 UQ16	5.20935393	0.02839927	9.334905	48.21	0.048	<u>A1</u>
13035	1989 UA6	3.97417007	0.16620234	3.640840	47.40	0.018	<u>A1</u>
11351	1997 TS25	5.26120450	0.06567781	11.570297	42.16	0.063	<u>A1</u>

**Table 6.** Number of the asteroids for which the size and albedo are estimated with AKARI and IRAS observations.  $N_{ID}$  indicates the number of the observations. They are divided into four categories by  $N_{ID} = 1$  or more with AKARI and IRAS (a, b, c, and d) as shown in Fig.13.

		IRAS	
		$N_{ID} \geq 2$	$N_{ID} = 1$
AKARI	$N_{ID} \geq 2$	1,961 (a)	97 (b)
	$N_{ID} = 1$	142 (c)	21 (d)

for the size and 0.8978 for the albedo for the asteroids observed twice or more (1,961 objects). However, there are several asteroids that show large discrepancies in their estimated size and albedo. We list these asteroids in Table 7. The albedo of 1166 Sakuntala is estimated as 0.65 from IRAS and  $0.19 \pm 0.01$  from AKARI observations. Because this asteroid is classified as S-type, whose typical albedo is 0.216 (or 0.158 in the Eight Color Asteroid Survey (ECAS) data (Zellner et al. 2009), see Table 8), the estimate with AKARI is more likely to be correct. Two asteroids 1384 Kniertje and 1444 Pannonia, have the albedo larger than 0.3 from IRAS but  $\sim 0.07$  from AKARI. Since these two asteroids are of C-type (the mean albedo of 0.073, or 0.045 in ECAS), IRAS observations seem to overestimate the albedo. The albedo of 5661 Hildebrand is estimated as 0.14 from IRAS and  $0.049 \pm 0.003$  from AKARI observations. Since this asteroid is a member of Hilda family composed of D-type asteroids (Dahlgren & Lagerkvist 1995) which suggests the low albedo, the AKARI result seems to be more likely than IRAS.

The discrepancy in the size estimate needs more detailed investigation. For 1 Ceres, the largest asteroid in the main belt or one of the dwarf planets, IRAS estimate the size as 850km and AKARI as  $970 \pm 13$ km. Hubble Space Telescope observations (Thomas et al. 2005) derive it as  $974.6 \times 909.4$ km, supporting the AKARI estimate. For the other 5 asteroids listed in upper rows of Table 7 only have sizes determined with IRAS and AKARI and thus it is difficult to conclude which would be more accurate. Further observations and measurements are needed to understand the discrepancy in size between IRAS and AKARI.

#### 4. Concluding remarks

We have created an unbiased, homogeneous asteroid catalog, which contains a total of 5,120 objects. This is the second generation asteroid survey after IRAS. The catalog revises the properties of several asteroids. The catalog will be publicly available via the Internet. This catalog will be significant for the various fields of the solar system science and contribute to future Rendezvous and/or sample return missions of small objects.

This study is based on observations with AKARI, a JAXA project with the participation of ESA. We would like to thank all the members of AKARI project for their

devoted efforts to achieve our observations. We are grateful to I. Yamamura for kindly providing us with the computer system including the web server for the public release of our catalog. Thanks are due to the referee, Simon Green, for careful reading and providing constructive suggestions, which have greatly helped to improve this paper. FU would like to thank C. P. Pearson for his helpful comments. SH is supported by the Space Plasma Laboratory, ISAS/JAXA. This work is supported in part by Grant-in-Aid for Scientific Research on Priority Areas No.19047003 to DK, Grant-in-Aid for Young Scientists (B) No.21740153 and Scientific Research on Innovative Areas No. 21111005 to TO, Grant-in-Aid for Scientific Research (C) No.19540251 to HK, and Grant-in-Aid for JSPS Fellows No.10J02063 to ST, from the Ministry of Education, Culture, Sports, Science and Technology of Japan.

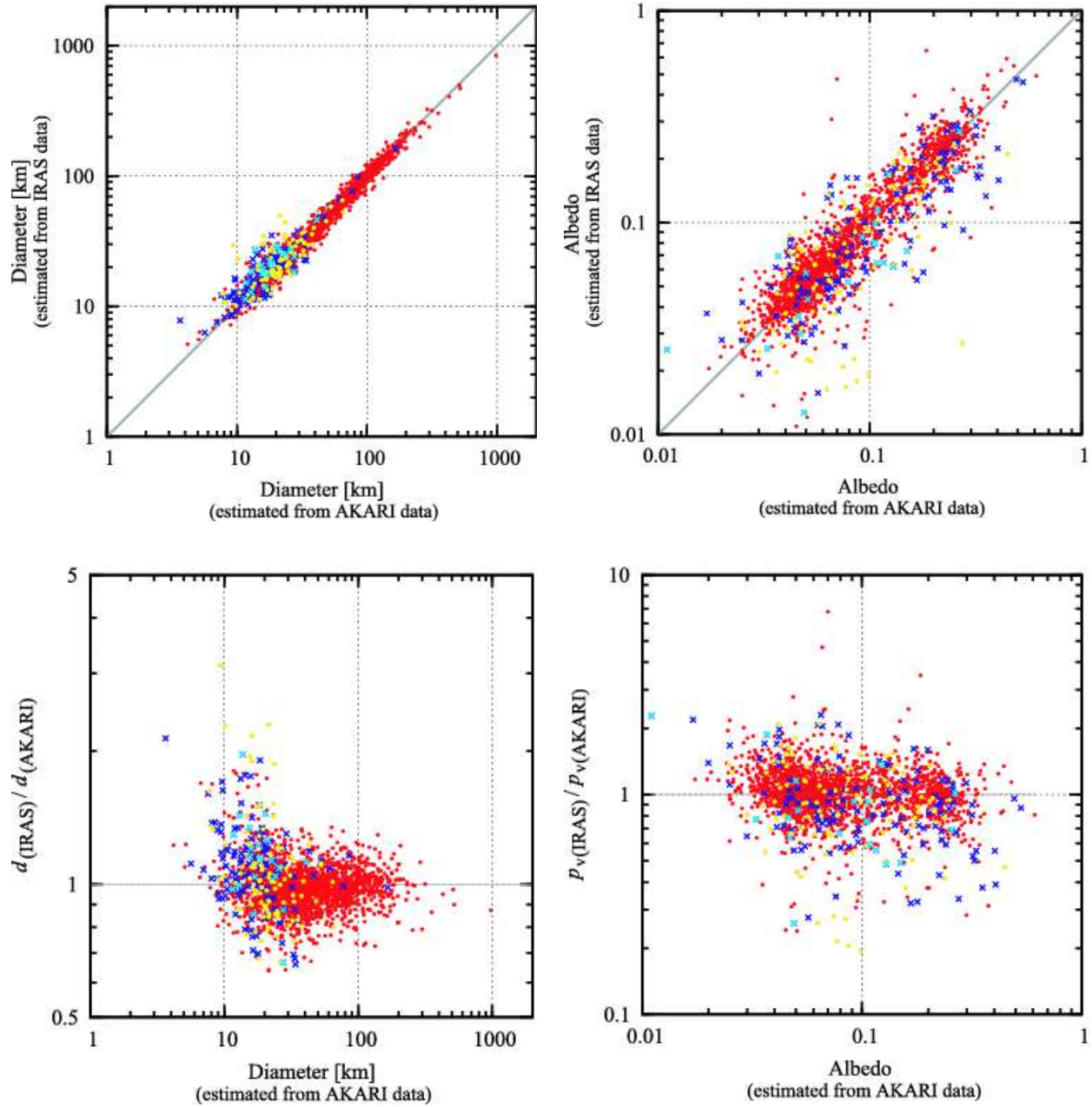


**Fig. 13.** Comparison between the estimates of AKARI and IRAS. The number of the objects for each observation is shown in Table 6. The red dots, the yellow dots, the blue cross, and the light blue cross indicate the asteroids of (a), (b), (c), and (d) in Table 6, respectively.

**Table 7.** Asteroids that show large discrepancy in the size and albedo estimated from IRAS and AKARI observations

Asteroid	IRAS data			AKARI data			taxonomic		
	$d$ [km]	$p_v$	$N_{ID}^\dagger$	$d$ [km]	$p_v$	$N_{ID}^\ddagger$	type	family	
(Asteroids with discrepant size)									
1293 Sonja	1933 SO	7.80	0.460	3	$3.65 \pm 0.45$	$0.529 \pm 0.133$	1	S	—
5356	1991 FF1	29.37	0.027	1	$9.39 \pm 0.70$	$0.273 \pm 0.044$	2	—	—
7875	1991 ES1	34.58	0.018	1	$15.95 \pm 0.45$	$0.087 \pm 0.005$	5	—	—
14409	1991 RM1	49.31	0.017	1	$21.45 \pm 0.88$	$0.077 \pm 0.007$	3	X(P)	—
16447 Vauban	1989 RX	23.10	0.019	1	$10.17 \pm 0.70$	$0.098 \pm 0.014$	2	—	—
(Asteroids with discrepant albedo)									
1166 Sakuntala	1930 MA	28.74	0.646	5	$26.32 \pm 0.39$	$0.185 \pm 0.006$	8	S	—
1384 Kniertje	1934 RX	27.51	0.308	8	$26.14 \pm 0.56$	$0.066 \pm 0.003$	7	C	Adeona
1444 Pannonia	1938 AE	29.20	0.475	2	$30.48 \pm 0.53$	$0.070 \pm 0.003$	7	C(B)	—
5661 Hildebrand	1977 PO1	34.37	0.136	2	$42.29 \pm 1.26$	$0.049 \pm 0.003$	5	—	Hilda

<sup>†</sup> The number of the observations used in the estimate of the albedo.

<sup>‡</sup> The number of the detections with *S9W* and *L18W*.

**Table 8.** Summary for 5 taxonomic classes of the asteroids detected with AKARI.

taxonomic type	AKARI			ECAS		
	number	$\overline{p_v}$	$\sigma(\overline{p_v})$	number	$\overline{p_v}$	$\sigma(\overline{p_v})$
C	616	0.073	0.043	62	0.045	0.010
S	614	0.216	0.086	78	0.158	0.038
X	418	0.106	0.101	52	0.126	0.027
D	165	0.075	0.051	20	0.031	0.005
V	5	0.296	0.113	1	0.249	—
total	1818			213		

Note: Current version of ECAS (Eight-Color Asteroid Survey; Zellner et al. 2009) contains not only the database of the reflectance spectrophotometric survey but also related dataset including the geometric albedo which we refer in this Table.

The mean albedo is taken as the average value of the taxonomic classes that belong to the same taxonomic type, i.e., C-type: B, C, F, and G; S-type: A, Q, R, and S; X-type: X, M, and P; D-type: D and T; and V-type: V.

Determination of the taxonomic classes for AKARI samples is based on the references summarized in Appendix 4:E1–E42.

## Appendix 1. Format of the AKARI/IRC Mid-infrared Asteroid Survey

The Asteroid Catalog Using Akari (AcuA) will be publicly available on the web server at the Institute of Space and Astronautical Science (ISAS), Japan Aerospace Exploration Agency (JAXA)<sup>2</sup>. It contains 5,120 asteroids detected in the mid-infrared with the size, albedo, and their associated uncertainties. It is in a standard ASCII file with a fixed-length record. Each line corresponds to each object with 10 columns. A summary of the format is given in Table 9. NUMBER, NAME, and PROV\_DES are the asteroid number, the name, and the provisional designation, which follow the formal assignment overseen by the IAU Minor Planet Center. HMAG and GPAR are the absolute magnitude and slope parameter taken from the Asteroid Orbital Elements Database of the Lowell obser-

vatory. NID gives the number of detections at *S9W* and *L18W* in total. DIAMETER and ALBEDO are the estimated size (diameter) and albedo, while D\_ERR, A\_ERR are their uncertainties estimated from the thermal model calculations. Users should note objects with single detection (NID=1). Example of the catalog data is shown in Table 10.

## Appendix 2. List of 55 asteroids used for thermal model calibration

We employ 55 well-studied main-belt asteroids (Müller 2005) to derive the best value for the beaming parameter  $\eta$  (Sect.2.2.4). Table 11 summarizes the calculation results of the 55 asteroids.

<sup>2</sup> <http://www.ir.isas.jaxa.jp/AKARI/Observation/> (not yet prepared at the time of submission to astro-ph)



**Table 9.** Format of the AKARI Asteroid catalog

Column	Format	Units	Label	Description
1 - 6	A6	—	NUMBER	Asteroid's number
8 - 25	A18	—	NAME	Asteroid's name
27 - 36	A10	—	PROV_DES	Asteroid's provisional designation
38 - 42	F5.2	mag	HMAG <sup>†</sup>	Absolute magnitude
44 - 48	F5.2	—	GPAR <sup>†</sup>	Slope parameter
50 - 51	I2	—	NID	Number of detections by AKARI
53 - 59	F7.2	km	DIAMETER	Mean diameter
61 - 65	F5.2	km	D_ERR	Uncertainty in diameter
67 - 71	F5.3	—	ALBEDO	Mean geometric albedo
73 - 77	F5.3	—	A_ERR	Uncertainty in albedo

<sup>†</sup> The H-G values are taken from the Asteroid Orbital Elements Database of the Lowell observatory.

**Table 10.** Example for the AcuA catalog data. Top 10 and bottom 10 asteroids in order of number and provisional designation of asteroids are listed.

NUMBER	NAME	PROV_DES	HMAG [mag]	GPAR	NID	DIAMETER [km]	D_ERR [km]	ALBEDO	A_ERR
1	Ceres		3.34	0.12	7	973.89	13.31	0.087	0.003
2	Pallas		4.13	0.11	12	512.59	4.98	0.150	0.004
3	Juno		5.33	0.32	8	231.09	2.60	0.246	0.007
4	Vesta		3.20	0.32	5	521.74	7.50	0.342	0.013
5	Astraea		6.85	0.15	7	110.77	1.37	0.263	0.008
6	Hebe		5.71	0.24	11	197.15	1.83	0.238	0.006
7	Iris		5.51	0.15	7	254.20	3.27	0.179	0.006
8	Flora		6.49	0.28	10	138.31	1.37	0.235	0.006
9	Metis		6.28	0.17	7	166.48	2.08	0.213	0.007
10	Hygiea		5.43	0.15	6	428.46	6.57	0.066	0.002
⋮	⋮	⋮	⋮	⋮	⋮	⋮	⋮	⋮	⋮
		2006 SE285	16.43	0.15	1	3.56	0.30	0.037	0.006
		2006 UD185	14.39	0.15	3	8.76	0.42	0.048	0.005
		2006 UL217	20.72	0.15	1	0.14	0.01	0.487	0.073
		2006 VV2	16.79	0.15	1	1.03	0.03	0.318	0.024
		2006 WT1	19.99	0.15	1	0.35	0.02	0.150	0.018
		2007 AG	20.11	0.15	6	0.33	0.01	0.158	0.008
		2007 BT2	17.06	0.15	3	2.76	0.14	0.038	0.004
		2007 DF8	20.32	0.15	2	0.47	0.02	0.059	0.006
		2007 FM3	16.87	0.15	5	3.14	0.13	0.033	0.003
		2007 HE15	19.60	0.15	1	0.37	0.02	0.182	0.021

**Table 11.** Results of the STM calculation for the 55 selected asteroids. The references of previous work are given in Appendix 3. The cited data refer to the underlined reference in the list.

Asteroid	type	detection with AKARI					previous work		References
		$N_{ID}$ S9W	$N_{ID}$ L18W	$N_{ID}$ total	$d$ [km]	$p_v$	$d$ [km]	$p_v$	
1 Ceres	C	3	4	7	973.89	0.087	959.60	0.096	A1, D2, D4, D5, D7, D8, D10, D16, D20, D26, D29, D33, D34, D42, D52, <u>D67</u>
2 Pallas	C	6	6	12	512.59	0.150	534.40	0.142	A1, D2, D5, D7, D15, D16, D20, D22, D26, D33, D42, D52, <u>D67</u>
3 Juno	S	4	4	8	231.09	0.246	233.92	0.238	<u>A1</u> , D2, D5, D26, D33, D42, D52
4 Vesta	V	2	3	5	521.74	0.342	548.50	0.317	A1, D1, D2, D3, D4, D5, D7, D8, D22, D25, D26, D33, D34, D42, D52, <u>D67</u>
6 Hebe	S	6	5	11	197.15	0.238	185.18	0.268	<u>A1</u> , D2, D16, D26, D34
7 Iris	S	3	4	7	254.20	0.179	199.83	0.277	<u>A1</u> , D3, D5, D15, D16, D26, D34, D42
8 Flora	S	4	6	10	138.31	0.235	135.89	0.243	<u>A1</u> , D3, D5, D26
9 Metis	D	4	3	7	166.48	0.213	154.67	0.228	<u>B1</u> , D3, D5, D42, D52, D55
10 Hygiea	C	3	3	6	428.46	0.066	469.30	0.056	A1, D3, D5, D16, D18, D22, D26, D33, D52, <u>D67</u>
12 Victoria	S	3	2	5	131.51	0.130	112.77	0.176	<u>A1</u> , D5, D7
17 Thetis	S	4	2	6	74.59	0.251	90.04	0.172	<u>A1</u> , D3, D5
18 Melpomene	S	3	3	6	139.95	0.225	140.57	0.223	<u>A1</u> , D3, D5, D34, D52
19 Fortuna	C	3	3	6	199.66	0.063	201.70	0.064	D3, D5, D7, D16, <u>D55</u>
20 Massalia	S	6	6	12	131.56	0.258	145.50	0.210	<u>A1</u> , D5, D7, D52
21 Lutetia	X	4	4	8	108.38	0.181	95.76	0.221	<u>A1</u> , D3, D5, D7, D59, D63
23 Thalia	S	1	3	4	106.21	0.260	107.53	0.254	<u>A1</u> , B1, D3, D5
24 Themis	C	4	4	8	176.81	0.084	176.20	0.084	D52, <u>D55</u>
28 Bellona	S	4	1	5	97.40	0.273	120.90	0.176	<u>A1</u> , B1, D5
29 Amphitrite	S	3	4	7	206.86	0.195	212.22	0.179	<u>A1</u> , D3, D5, D26
31 Euphrosyne	C	6	6	12	276.49	0.047	255.90	0.054	<u>A1</u>
37 Fides	S	3	3	6	103.23	0.204	108.35	0.183	<u>A1</u> , D3, D5
40 Harmonia	S	3	5	8	110.30	0.233	107.62	0.242	<u>A1</u> , D3, D5, D52
41 Daphne	C	3	4	7	179.61	0.078	174.00	0.083	<u>A1</u> , D7
42 Isis	S	4	3	7	104.50	0.158	100.20	0.171	<u>A1</u> , D7
47 Aglaja	C	2	1	3	147.05	0.060	126.96	0.080	<u>A1</u> , D5
48 Doris	C	3	4	7	200.27	0.077	221.80	0.062	<u>A1</u>
52 Europa	C	4	3	7	350.36	0.043	302.50	0.058	<u>A1</u> , D5, D7, D26
54 Alexandra	C	3	5	8	144.46	0.074	165.75	0.056	<u>A1</u> , D5, D7, D33, D52
56 Melete	X	4	6	10	105.22	0.076	113.24	0.065	<u>A1</u> , D5, D16
65 Cybele	X	4	2	6	300.54	0.044	237.26	0.071	<u>A1</u> , D16, D26, D33
69 Hesperia	X	5	4	9	132.74	0.157	138.13	0.140	<u>A1</u>
85 Io	C	4	4	8	150.66	0.071	154.79	0.067	<u>A1</u> , D7
88 Thisbe	C	3	4	7	195.59	0.071	200.58	0.067	<u>A1</u>
93 Minerva	C	3	3	6	147.10	0.068	141.55	0.073	<u>A1</u> , B1
94 Aurora	C	2	2	4	179.15	0.053	204.89	0.040	<u>A1</u> , D5, D7
106 Dione	C	3	3	6	153.42	0.084	146.59	0.089	<u>A1</u> , D7, D33
165 Loreley	C	4	2	6	173.66	0.051	154.78	0.064	<u>A1</u>
173 Ino	X	3	1	4	160.61	0.059	154.10	0.064	<u>A1</u>
196 Philomela	S	2	4	6	141.78	0.213	136.39	0.230	<u>A1</u> , D5, D7
230 Athamantis	S	4	5	9	108.28	0.173	108.99	0.171	<u>A1</u> , D3, D5, D7
241 Germania	C	3	3	6	181.57	0.050	168.90	0.058	<u>A1</u> , D5
283 Emma	C	4	8	12	122.07	0.039	148.06	0.026	<u>A1</u>
313 Chaldaea	C	4	4	8	94.93	0.054	96.34	0.052	<u>A1</u> , D5, D8, D33
334 Chicago	C	4	5	9	167.21	0.057	158.55	0.062	<u>A1</u>
360 Carlova	C	4	4	8	121.52	0.049	115.76	0.053	<u>A1</u> , D5, D7
372 Palma	C	2	4	6	177.21	0.075	188.62	0.066	<u>A1</u>
423 Diotima	C	5	1	6	226.91	0.049	208.77	0.051	<u>A1</u>
451 Patientia	C	5	5	10	234.91	0.071	224.96	0.076	<u>A1</u> , D5, D7, D16
471 Papagena	S	3	3	6	117.44	0.261	134.19	0.199	<u>A1</u> , D3
505 Cava	C	5	4	9	100.55	0.063	115.80	0.040	<u>D55</u>
511 Davida	C	4	3	7	290.98	0.070	326.06	0.054	<u>A1</u> , D2, D3, D7, D52
532 Herculina	S	4	2	6	216.77	0.184	222.39	0.169	<u>A1</u> , D3, D5, D8, D33, D42
690 Wratislavia	C	2	4	6	158.11	0.044	134.65	0.060	<u>A1</u>
704 Interamnia	C	7	4	11	316.25	0.075	316.62	0.074	<u>A1</u> , D5, D7, D52
776 Berbericia	C	4	5	9	149.76	0.067	151.17	0.066	<u>A1</u>

**Appendix 3. Reference list of previous work of The Infrared Astronomy Satellite (IRAS): the size and albedo of asteroids**

(A1) Tedesco et al. 2002a.

The references of previous work are given in the following list. The Midcourse Space Experiment (MSX)

(B1) Tedesco et al. 2002b.

## The Spitzer Space Telescope (SST):

- |                               |                            |
|-------------------------------|----------------------------|
| (C1) Stansberry et al. 2008   | (C2) Trilling et al. 2008  |
| (C3) Ryan et al. 2009         | (C4) Campins et al. 2009a  |
| (C5) Campins et al. 2009b     | (C6) Fernández et al. 2009 |
| (C7) Harris et al. 2009       | (C8) Licandro et al. 2009  |
| (C9) Bhattacharya et al. 2010 | (C10) Trilling et al. 2010 |

Other work including the Infrared Space Observatory (ISO) and ground-based observatories in the chronological order:

## \* 1970–1979

- |                             |                                 |
|-----------------------------|---------------------------------|
| (D1) Allen 1970             | (D2) Cruikshank & Morrison 1973 |
| (D3) Morrison 1974          | (D4) Gillett & Merrill 1975     |
| (D5) Hansen 1976            | (D6) Cruikshank & Jones 1977    |
| (D7) Morrison 1977a         | (D8) Gradie 1978                |
| (D9) Lebofsky et al. 1978   | (D10) Stier & Traub 1978        |
| (D11) Lebofsky & Rieke 1979 |                                 |

## \* 1980–1989

- |                            |                                      |
|----------------------------|--------------------------------------|
| (D12) Lebofsky et al. 1981 | (D13) Hamilton Brown & Morrison 1984 |
| (D14) Lebofsky et al. 1984 | (D15) LeVan & Price 1984             |
| (D16) Green et al. 1985a   | (D17) Green et al. 1985b             |
| (D18) Lebofsky et al. 1985 | (D19) Vilas et al. 1985              |
| (D20) Lebofsky et al. 1986 | (D21) Tedesco & Gradie 1987          |
| (D22) Johnston et al. 1989 | (D23) Veeder et al. 1989             |

## \* 1990–1999

- |                              |                              |
|------------------------------|------------------------------|
| (D24) Cruikshank et al. 1991 | (D25) Redman et al. 1992     |
| (D26) Altenhoff et al. 1994  | (D27) Altenhoff et al. 1995  |
| (D28) Campins et al. 1995    | (D29) Altenhoff et al. 1996  |
| (D30) Mottola et al. 1997    | (D31) Harris et al. 1998     |
| (D32) Jewitt & Kalas 1998    | (D33) Müller & Lagerros 1998 |
| (D34) Redman et al. 1998     | (D35) Harris & Davies 1999   |

## \* 2000–2009

- |                              |                             |
|------------------------------|-----------------------------|
| (D36) Thomas et al. 2000     | (D37) Altenhoff et al. 2001 |
| (D38) Fernández et al. 2001  | (D39) Harris et al. 2001    |
| (D40) Jewitt et al. 2001     | (D41) Fernández et al. 2002 |
| (D42) Müller et al. 2002     | (D43) Tedesco & Desert 2002 |
| (D44) Delbó et al. 2003      | (D45) Fernández et al. 2003 |
| (D46) Delbó 2004             | (D47) Müller et al. 2004    |
| (D48) Cruikshank et al. 2005 | (D49) Fernández et al. 2005 |
| (D50) Harris et al. 2005     | (D51) Kraemer et al. 2005   |
| (D52) Lim et al. 2005        | (D53) Müller et al. 2005    |
| (D54) Rivkin et al. 2005     | (D55) Tedesco et al. 2005   |
| (D56) Wolters et al. 2005    | (D57) Delbó et al. 2006     |
| (D58) Emery et al. 2006      | (D59) Müller et al. 2006    |
| (D60) Harris et al. 2007     | (D61) Müller et al. 2007    |
| (D62) Trilling et al. 2007   | (D63) Carvano et al. 2008   |
| (D64) Hasegawa et al. 2008   | (D65) Wolters et al. 2008   |
| (D66) Delbó et al. 2009      | (D67) Hormuth & Müller 2009 |

- |                                    |                                    |
|------------------------------------|------------------------------------|
| (E1) Jewitt & Luu 1990             | (E2) Barucci & Lazzarin 1993       |
| (E3) Dahlgren & Lagerkvist 1995    | (E4) Xu et al. 1995                |
| (E5) Dahlgren et al. 1997          | (E6) di Martino et al. 1997        |
| (E7) Lazzarin et al. 1997          | (E8) Doressoundiram et al. 1998    |
| (E9) Hicks et al. 1998             | (E10) Hicks et al. 2000            |
| (E11) Zappalà et al. 2000          | (E12) Binzel et al. 2001           |
| (E13) Cellino et al. 2001          | (E14) Fornasier & Lazzarin 2001    |
| (E15) Le Bras et al. 2001          | (E16) Manara et al. 2001           |
| (E17) Mothé-Diniz et al. 2001      | (E18) Fornasier et al. 2003        |
| (E19) Rivkin et al. 2003           | (E20) Yang et al. 2003             |
| (E21) Bendjoya et al. 2004         | (E22) Binzel et al. 2004           |
| (E23) Duffard et al. 2004          | (E24) Fornasier et al. 2004        |
| (E25) Marchi et al. 2004           | (E26) Lazzarin et al. 2004a        |
| (E27) Lazzarin et al. 2004b        | (E28) Lagerkvist et al. 2005       |
| (E29) Lazzarin et al. 2005         | (E30) Marchi et al. 2005           |
| (E31) Alvarez-Candal et al. 2006   | (E32) Dotto et al. 2006            |
| (E33) de León et al. 2006          | (E34) Michelsen et al. 2006        |
| (E35) Davies et al. 2007           | (E36) Licandro et al. 2008         |
| (E37) Moskovitz et al. 2008a       | (E38) Moskovitz et al. 2008b       |
| (E39) Mothé-Diniz & Nesvorný 2008a | (E40) Mothé-Diniz & Nesvorný 2008b |
| (E41) Roig et al. 2008             | (E42) Duffard & Roig 2009          |

#### Appendix 4. Reference list of previous work of the taxonomic types of asteroids

The references of previous work used for determining the taxonomic classifications (based on the definitions by Tholen (1984), Bus (1999), and Lazzaro et al. (2004)) described in Table 8 are given in the following list.

## References

- Allen, D. A. 1970, *Nature*, 227, 158
- Allen, D. A. 1971, *The Method of Determining Infrared Diameters*, in *Physical Studies of Minor Planets*, ed. T. Gehrels (Washington: National Aeronautics and Space Administration SP-267), 41
- Altenhoff, W. J., Johnston, K. J., Stumpff, P., & Webster, W. J. 1994, *A&A*, 287, 641
- Altenhoff, W. J., & Stumpff, P. 1995, *A&A*, 293, L41
- Altenhoff, W. J., Baars, J. W. M., Schraml, J. B., Stumpff, P., & von Kap-Herr, A. 1996, *A&A*, 309, 953
- Altenhoff, W. J., Menten, K. M., & Bertoldi, F. 2001, *A&A*, 366, L9
- Alvarez-Candal, A., Duffard, R., Lazzaro, D., & Michtchenko, T. 2006, *A&A*, 459, 969
- Barucci, M. A., & Lazzarin, M. 1993, *Planetary and Space Science*, 41, 641
- Bendjoya, P., Cellino, A., di Martino, M., & Saba, L. 2004, *Icarus*, 168, 374
- Bhattacharya, B., et al. 2010, *ApJ*, 720, 114
- Binzel, R. P., Harris, A. W., Bus, S. J., & Burbine, T. H. 2001, *Icarus*, 151, 139
- Binzel, R. P., Rivkin, A. S., Stuart, J. S., Harris, A. W., Bus, S. J., & Burbine, T. H. 2004, *Icarus*, 170, 259
- Bottke, W. F., Durda, D. D., Nesvorný, D., Jedicke, R., Morbidelli, A., Vokrouhlický, D., & Levison, H. F. 2005, *Icarus*, 179, 63
- Bowell, E., Hapke, B., Domingue, D., Lumme, K., Peltoniemi, J., & Harris, A. W. 1989, *Application of photometric models to asteroids*, in *Asteroids II*, ed. R. P. Binzel, T. Gehrels, & M. S. Matthews (Tucson: University of Arizona Press), 524
- Bowell, E., Muinonen, K., & Wasserman, L. H. 1994, *A Public-Domain Asteroid Orbit Data Base*, in *Asteroids, comets, meteors 1993*, ed. A. Milani, M. di Martino, & A. Cellino (Dordrecht: Kluwer Academic Publishers), 477
- Britt, D. T., Yeomans, D., Housen, K., & Consolmagno, G. 2002, *Asteroid Density, Porosity, and Structure*, in *Asteroids III*, ed. W. F. Bottke, A. Cellino, P. Paolicchi, & R. P. Binzel, (Tucson: University of Arizona Press), 485
- Burbine, T. H., Rivkin, A. S., Noble, S. K., Mothé-Diniz, T., Bottke, W. F., McCoy, T. J., Dyar, M. D., & Thomas, C. A. 2008, *Reviews in Mineralogy & Geochemistry*, 68, 273
- Bus, S. J. 1999, *Compositional structure in the asteroid belt: Results of a spectroscopic survey*, Ph.D. thesis, Massachusetts Institute of Technology, Boston
- Campins, H., Osip, D. J., Rieke, G. H., & Rieke, M. J. 1995, *Planetary and Space Science*, 43, 733
- Campins, H., Emery, J. P., Kelley, M. S., Fernández, Y., Licandro, J., Delbó, M., Barucci, A., & Dotto, E. 2009a, *A&A*, 503, L17
- Campins, H., Kelley, M. S., Fernández, Y., Licandro, J., & Hargrove, K. 2009b, *Earth, Moon, and Planets*, 105, 159
- Carvano, J. M., Barucci, M. A., Delbó, M., Fornasier, S., Lowry, S., & Fitzsimmons, A. 2008, *A&A*, 479, 241
- Cellino, A., Zappalà, V., Doressoundiram, A., di Martino, M., Bendjoya, Ph., Dotto, E., & Migliorini, F. 2001, *Icarus*, 152, 225
- Christensen, E. J. et al. 2006, *Minor Planet Electronic Circular 2006-S16 : 2006 SA6* (issued 2006 September 18)
- Cruikshank, D. P., & Morrison, D. 1973, *Icarus*, 20, 477
- Cruikshank, D. P., & Jones, T. J. 1977, *Icarus*, 31, 427
- Cruikshank, D. P., Tholen, D. J., Bell, J. F., Hartmann, W. K., & Brown, R. H. 1991, *Icarus*, 89, 1
- Cruikshank, D. P., Stansberry, J. A., Emery, J. P., Fernández, Y. R., Werner, M. W., Trilling, D. E., & Rieke, G. H. 2005, *ApJ*, 624, L53
- Dahlgren, M., & Lagerkvist, C.-I. 1995, *A&A*, 302, 907
- Dahlgren, M., Lagerkvist, C.-I., Fitzsimmons, A., Williams, I. P., & Gordon, M. 1997, *A&A*, 323, 606
- Davies, J. K., Harris, A. W., Rivkin, A. S., Wolters, S. D., Green, S. F., McBride, N., Mann, R. K., & Kerr, T. H. 2007, *Icarus*, 186, 111
- de León, J., Licandro, J., Duffard, R., & Serra-Ricart, M. 2006, *Advances in Space Research*, 37, 178
- Delbó, M., Harris, A. W., Binzel, R. P., Pravec, P., & Davies, J. K. 2003, *Icarus*, 166, 116
- Delbó, M. 2004, *The nature of near-earth asteroids from the study of their thermal infrared emission*, Ph.D. thesis, Freie Universität Berlin <sup>3</sup>
- Delbó, M., et al. 2006, *Icarus*, 181, 618
- Delbó, M., Ligori, S., Matter, A., Cilino, A., & Berthier, J. 2009, *ApJ*, 694, 1228
- di Martino, M., Migliorini, F., Zappalà, V., Manara, A., & Barbieri, C. 1997, *Icarus*, 127, 112
- Doressoundiram, A., Barucci, M. A., Fulchignoni, M., & Florczak, M. 1998, *Icarus*, 131, 15
- Dormand, J. R., El-Mikkawy, M. E. A., & Prince, P. J. 1987, *High-Order Embedded Runge-Kutta-Nystrom Formulae*, *IMA Journal of Numerical Analysis*, Volume 7, Issue 4, 423
- Dotto, E., et al. 2006, *Icarus*, 183, 420
- Duffard, R., Lazzaro, D., Licandro, J., de Sanctis, M. C., Capria, M. T., & Carvano, J. M. 2004, *Icarus*, 171, 120
- Duffard, R., & Roig, F. 2009, *Planetary and Space Science*, 57, 229
- Emery, J. P., Cruikshank, D. P., & van Cleve, J. 2006, *Icarus*, 182, 496
- Fernández, Y. R., Jewitt, D. C., & Sheppard, S. S. 2001, *ApJ*, 553, L197
- Fernández, Y. R., Jewitt, D. C., & Sheppard, S. S. 2002, *AJ*, 123, 1050
- Fernández, Y. R., Sheppard, S. S., & Jewitt, D. C. 2003, *AJ*, 126, 1563
- Fernández, Y. R., Jewitt, D. C., & Sheppard, S. S. 2005, *AJ*, 130, 308
- Fernández, Y. R., Jewitt, D. C., & Ziffer, J. E. 2009, *AJ*, 138, 240
- Fornasier, S., & Lazzarin, M. 2001, *Icarus*, 152, 127
- Fornasier, S., et al. 2003, *A&A*, 398, 327
- Fornasier, S., Dotto, E., Marzari, F., Barucci, M. A., Boehnhardt, H., Hainaut, O., & de Bergh, C. 2004, *Icarus*, 172, 221
- Fowler, J. W., & Chillemi, J. R. 1992, *IRAS asteroid data processing*, in *The IRAS Minor Planet Survey*, Phillips Laboratory, Hanscom Air Force Base, MA, p.17
- Gillett, F. C., & Merrill, K. M. 1975, *Icarus*, 26, 358
- Gladman, B. J., et al. 2009, *Icarus*, 202, 104
- Gradie, J.C. 1978, *An astrophysical study of the minor planets in the EOS and Koronis asteroid families*, Ph.D. thesis, Arizona University, Tucson
- Green, S. F., Eaton, N., Aitken, D. K., Roche, P. F., & Meadows, A. J. 1985a, *Icarus*, 62, 282
- Green, S. F., Meadows, A. J., & Davies, J. K. 1985b, *MNRAS*, 214, 29

<sup>3</sup> [http://sbn.psi.edu/pds/asteroid/EAR\\_A\\_KECK1LWS\\_ETAL\\_5\\_DELBO\\_V1\\_0/](http://sbn.psi.edu/pds/asteroid/EAR_A_KECK1LWS_ETAL_5_DELBO_V1_0/)



- Hamilton Brown, R., & Morrison, D. 1984, *Icarus*, 59, 20
- Hansen, O. L. 1976, *AJ*, 81, 74
- Harris, A. W., Davies, J. K., & Green, S. F. 1998, *Icarus*, 135, 441
- Harris, A. W. & Davies, J. K. 1999, *Icarus*, 142, 464
- Harris, A. W., Delbó, M., Binzel, R. P., Davies, J. K., Roberts, J., Tholen, D. J., & Whiteley, R. J. 2001, *Icarus*, 153, 332
- Harris, A. W. & Lagerros, J. S. V. 2002, Asteroids in the Thermal Infrared, in Asteroids III, ed. W. F. Bottke, A. Cellino, P. Paolicchi, & R. P. Binzel, (Tucson: University of Arizona Press), 205
- Harris, A. W., Müller, M., Delbó, M. J., & Bus, S. J. 2005, *Icarus*, 179, 95
- Harris, A. W., Müller, M., Delbó, M. J., & Bus, S. J. 2007, *Icarus*, 188, 414
- Harris, A. W., Müller, M., Lisse, C. M., & Cheng, A. F. 2009, *Icarus*, 199, 86
- Hasegawa, S., Müller, T. G., Kawakami, K., Kasuga, T., Wada, T., Ita, Y., Takato, N., Terada, H., Fujiyoshi, T., & Abe, M. 2008, *PASJ*, 60, S399
- Hicks, M. D., Fink, U., & Grundy, W. M. 1998, *Icarus*, 133, 69
- Hicks, M. D., Buratti, B. J., Newburn, R. L., & Rabinowitz, D. L. 2000, *Icarus*, 143, 354
- Hicks, M. D., & Bauer, J. M. 2007, *ApJ*, 662, L47
- Hilton, J. L. 2002, Asteroid Masses and Densities, in Asteroids III, ed. W. F. Bottke, A. Cellino, P. Paolicchi, & R. P. Binzel, (Tucson: University of Arizona Press), 103
- Hormuth, F., & Müller, T. G. 2009, *A&A*, 497, 983
- Ishihara, D., et al. 2010, *A&A*, 514, A1
- Jewitt, D., & Luu, J. X. 1990, *AJ*, 100, 933
- Jewitt, D., & Kalas, P. 1998, *ApJ*, 499, L103
- Jewitt, D., Aussel, H., & Evans, A. 2001, *Nature*, 411, 446
- Johnston, K. J., Lamphear, E. J., Webster, W. J., Lowman, P. D., Seidelmann, P. K., Kaplan, G. H., Wade, C. M., & Hobbs, R. W. 1989, *AJ*, 89, 335
- Kataza, H., et al. 2010, AKARI/IRC All-Sky Survey Point Source Catalogue Version 1.0 Release Note <sup>4</sup>
- Kawada, M., et al. 2007, *PASJ*, 59, S389
- Kessler, M. F., et al. 1996, *A&A*, 315, L27
- Kowalski, R. A. et al. 2007, Minor Planet Electronic Circular 2007-F51 : 2007 FM3 (issued 2007 March 21)
- Kraemer, K. E., Lisse, C. M., Price, S. D., Mizuno, D., Walker, R. G., Farnham, T. L., & Makinen, T. 2005, *AJ*, 130, 2363
- Lagerkvist, C.-I., Moroz, L., Nathues, A., Erikson, A., Lahulla, F., Karlsson, O., & Dahlgren, M. 2005, *A&A*, 432, 349
- Lazzarin, M., di Martino, M., Barucci, M. A., Doressoundiram, A., & Florczak, M. 1997, *A&A*, 327, 388
- Lazzarin, M., Marchi, S., Barucci, M. A., di Martino, & M., Barbieri, C. 2004a, *Icarus*, 169, 373
- Lazzarin, M., Marchi, S., Magrin, S., & Barbieri, C. 2004b, *Memorie della Società Astronomica Italiana Supplement*, 5, 21
- Lazzarin, M., Marchi, S., Magrin, S., & Licandro, J. 2005, *MNRAS*, 359, 1575
- Lazzaro, D., Angeli, C. A., Carvano, J. M., Mothé-Diniz, T., Duffard, R., & Florczak, M. 2004, *Icarus*, 172, 179
- Le Bras, A., Dotto, E., Fulchignoni, M., Doressoundiram, A., Barucci, M. A., Le Mouélic, S., Forni, O., & Quirico, E. 2001, *A&A*, 379, 660
- Lebofsky, L. A., Veeder, G. J., Lebofsky, M. J., & Matson, D. L. 1978, *Icarus*, 35, 336
- Lebofsky, L. A., & Rieke, G. H. 1979, *Icarus*, 40, 297
- Lebofsky, L. A., Veeder, G. J., Rieke, G. H., Lebofsky, M. T., Matson, D. L., Kowal, C., Wynn-Williams, C. G., & Becklin, E. E. 1981, *Icarus*, 48, 335
- Lebofsky, L. A., Tholen, D. J., Rieke, G. H., & Lebofsky, M. J. 1984, *Icarus*, 60, 532
- Lebofsky, L. A., et al. 1985, *Icarus*, 63, 192
- Lebofsky, L. A., et al. 1986, *Icarus*, 68, 239
- Lebofsky, L. A., & Spencer, J. R. 1989, Radiometry and thermal modeling of asteroids, in Asteroids II, ed. R. P. Binzel, T. Gehrels, & M. S. Matthews (Tucson: University of Arizona Press), 128
- LeVan, P. D., & Price, S. D. 1984, *Icarus*, 57, 35
- Licandro, J., Alvarez-Candal, A., de León, J., Pinilla-Alonso, N., Lazzaro, D., & Campins, H. 2008, *A&A*, 481, 861
- Licandro, J., et al. 2009, *A&A*, 507, 1667
- Lim, L. F., McConnochie, T. H., Bell, J. F., & Hayward, T. L. 2005, *Icarus*, 173, 385
- Lowry, S. C., Fitzsimmons, A., Hicks, M. D., Lawrence, K., & Forti, G. 2006, *IAU Circ.*, 8735
- Manara, A., Covino, S., & di Martino, M. 2001, *Revista Mexicana de Astronomia y Astrofísica*, 37, 35
- Marchi, S., Lazzarin, M., & Magrin, S. 2004, *A&A*, 420, L5
- Marchi, S., Lazzarin, M., Paolicchi, P., & Magrin, S. 2005, *Icarus*, 175, 170
- Matson, D. L. 1971, Infrared Observations of Asteroids, in Physical Studies of Minor Planets, ed. T. Gehrels (Washington: National Aeronautics and Space Administration SP-267), 45
- Michelsen, R., Nathues, A., & Lagerkvist, C.-I. 2006, *A&A*, 451, 331
- Mill, J. D., et al. 1994, Midcourse space experiment: Introduction to the spacecraft, instruments, and scientific objectives, *Journal of Spacecraft and Rockets*, vol. 31, no. 5, 900
- Morrison, D. 1974, *ApJ*, 194, 203
- Morrison, D. 1977a, *ApJ*, 214, 667
- Morrison, D. 1977b, *Icarus*, 31, 185
- Moskovitz, N. A., Jedicke, R., Gaidos, E., Willman, M., Nesvorný, D., Fevig, R., & Ivezić, Ž. 2008a, *Icarus*, 198, 77
- Moskovitz, N. A., Lawrence, S., Jedicke, R., Willman, M., Haghhighipour, N., Bus, S. J., & Gaidos, E. 2008b, *ApJ*, 682, L57
- Mothé-Diniz, T., di Martino, M., Bendjoya, P., Doressoundiram, A., & Migliorini, F. 2001, *Icarus*, 152, 117
- Mothé-Diniz, T., & Nesvorný, D. 2008a, *A&A*, 486, L9
- Mothé-Diniz, T., & Nesvorný, D. 2008b, *A&A*, 492, 593
- Mottola, S., et al. 1997, *AJ*, 114, 1234
- Müller, T. G. & Lagerros, J. S. V. 1998, *A&A*, 338, 340
- Müller, T. G., Hotzel, S., & Stickel, M. 2002, *A&A*, 389, 665
- Müller, T. G., Sterzik, M. F., Schütz, O., Pravec, P., & Siebenmorgen, R. 2004, *A&A*, 424, 1075
- Müller, T. G., Sekiguchi, T., Kaasalainen, M., Abe, M., & Hasegawa, S. 2005, *A&A*, 443, 347
- Müller, T. G. 2005, The Asteroid Preparatory Programme for Herschel, Astro-F and ALMA, in the Proceedings of “the dusty and molecular universe: a prelude to Herschel and ALMA”, ed. A. Wilson (Noordwijk, Netherlands: ESA SP-577), 471
- Müller, M., Harris, A. W., Bus, S. J., Hora, J. L., Kassis, M., & Adams, J. D. 2006, *A&A*, 447, 1153

<sup>4</sup> <http://www.ir.isas.jaxa.jp/AKARI/Observation/PSC/Public/RN/AKARI-IRC.PSC-V1.RN.pdf>

- Müller, M., Harris, A. W., & Fitzsimmons, A. 2007, *Icarus*, 187, 611
- Murakami, H., et al. 2007, *PASJ*, 59, S369
- Neugebauer, G., et al. 1984, *ApJ*, 278, L1
- Onaka, T., et al. 2007, *PASJ*, 59, S401
- Parker, A., Ivezić, Ž, Jurić, M., Lupton, R., Sekora, M. D., & Kowalski, A. 2008, *Icarus*, 198, 138
- Price, S. D., Egan, M. P., Carey, S. J., Mizuno, D. R., & Kuchar, T. A. 2001, *AJ*121, 2819
- Redman, R. O., Feldman, P. A., Matthews, H. E., Halliday, I., & Creutzberg, F. 1992, *AJ*, 104, 405
- Redman, R. O., Feldman, P. A., & Matthews, H. E. 1998, *AJ*, 116, 1478
- Rivkin, A. S., Binzel, R. P., Howell, E. S., Bus, S. J., & Grier, J. A. 2003, *Icarus*, 165, 349
- Rivkin, A. S., Binzel, R. P., & Bus, S. J. 2005, *Icarus*, 175, 175
- Roig, F., Nesvorný, D., Gil-Hutton, R., & Lazzaro, D. 2008, *Icarus*, 194, 125
- Ryan, E. L., et al. 2009, *AJ*, 137, 5134
- Stansberry, J., Grundy, W., Brown, M., Cruikshank, D. P., Spencer, J., Trilling, D., & Margot, J.-L. 2008, Physical properties of Kuiper belt and Centaurs objects: Constraint from Spitzer Space Telescope, in *The solar system beyond Neptune*, ed. M. A. Barucci, H. Boehnhardt, D. P. Cruikshank, & A. Morbidelli (Tucson: University of Arizona Press), 161
- Stier, M. T., & Traub, W. A. 1978, *ApJ*, 226, 347
- Sykes, M. V., Cutri, R. M., Fowler, J. W., Tholen, D. J., Skrutskie, M. F., Price, S., & Tedesco, E. F. 2000, *Icarus*, 146, 161
- Tedesco, E. F., & Gradie, J. D. 1987, *AJ*, 93, 738
- Tedesco, E. F., Noah P. V., Noah, M., & Price, S. D. 2002a, *AJ*, 123, 1056 (The actual data is available at NASA Planetary Data System, Supplemental IRAS Minor Planet Survey (SIMPS) <sup>5</sup>)
- Tedesco, E. F., & Desert, F.-X. 2002, *AJ*, 123, 2070
- Tedesco, E. F., Egan, M. P., & Price, S. D. 2002b, *AJ*, 124, 583 (The actual data is available at NASA Planetary Data System, MSX Infrared Minor Planet Survey <sup>6</sup>)
- Tedesco, E. F., Cellino, A., & Zappalà, V. 2005, *AJ*, 129, 2869 (The actual data is available at NASA Planetary Data System, Statistical Asteroid Model, Version 1.0 (SAM-I) <sup>7</sup>)
- Tholen, D. J. 1984, Asteroid taxonomy from cluster analysis of Photometry, Ph.D. thesis, Arizona University, Tucson
- Thomas, N., et al. 2000, *ApJ*, 534, 446
- Thomas, P. C., Parker, J. Wm., McFadden, L. A., Russell, C. T., Stern, S. A., Sykes, M. V., & Young, E. F. 2005, *Nature*, 437, 224
- Trilling, D. E., Rivkin, A. S., Stansberry, J. A., Spahr, T. B., Crudo, R. A., & Davies, J. K. 2007, *Icarus*, 192, 442
- Trilling, D. E., et al. 2008, *ApJ*, 683, L199
- Trilling, D. E., et al. 2010, *AJ*, 140, 770
- Veeder, G. J., Hanner, M. S., Matson, D. L., Tedesco, E. F., Lebofsky, L. A., & Tokunaga, A. T. 1989, *AJ*, 97, 1211
- Vilas, F., Tholen, D. J., Lebofsky, L. A., Campins, H., Veeder, G. J., Binzel, R. P., & Tokunaga, A. T. 1985, *Icarus*, 63, 201
- Warner, B. D., Harris, A. W., & Pravec, P. 2009, *Icarus*, 202, 134
- Wolters, S. D., Green, S. F., McBride, N., & Davies, J. K. 2005, *Icarus*, 175, 92
- Wolters, S. D., Green, S. F., McBride, N., & Davies, J. K. 2008, *Icarus*, 193, 535
- Xu, S., Binzel, R. P., Burbine, T. H., & Bus, S. J. 1995, *Icarus*, 115, 1
- Yang, B., Zhu, J., Gao, J., Ma, J., Zhou, X., Wu, H., & Guan, M. 2003, *AJ*, 126, 1086
- Yoshida, F., & Nakamura, T. 2007, *Planetary and Space Science*, 55, 1113
- Zappalà, V., Bendjoya, Ph., Cellino, A., di Martino, M., Doressoundiram, A., Manara, A., & Migliorini, F. 2000, *Icarus*, 145, 4
- Zellner, B., Tholen, D. J., Tedesco, E. F. 2009, Eight Color Asteroid Survey V4.0, NASA Planetary Data System, EAR-A-2CP-3-RDR-ECAS-V4.0 <sup>8</sup>

<sup>5</sup> [http://sbn.psi.edu/pds/asteroid/IRAS\\_A\\_FPA\\_3\\_RDR\\_IMPS\\_V6\\_0/](http://sbn.psi.edu/pds/asteroid/IRAS_A_FPA_3_RDR_IMPS_V6_0/)

<sup>6</sup> [http://sbn.psi.edu/pds/asteroid/MSX\\_A\\_SPIRIT3\\_5\\_SBN0003\\_MIMPS\\_V1\\_0/](http://sbn.psi.edu/pds/asteroid/MSX_A_SPIRIT3_5_SBN0003_MIMPS_V1_0/)

<sup>7</sup> <http://sbn.psi.edu/pds/SAM-I/>

<sup>8</sup> [http://sbn.psi.edu/pds/asteroid/EAR\\_A\\_2CP\\_3\\_RDR\\_ECAS\\_V4\\_0/](http://sbn.psi.edu/pds/asteroid/EAR_A_2CP_3_RDR_ECAS_V4_0/)